Reduced-Order Models: Convergence Between Data and Simulation

Angelo Iollo

Michel Bergmann, Andrea Ferrero, Sébastien Riffaud

INRIA Bordeaux Sud-Ouest - MEMPHIS team
Institut de Mathématiques de Bordeaux

Edoardo Lombardi, Angela Scardigli, Haysam Telib

Optimad Engineering - Torino

angelo.iollo@inria.fr
https://team.inria.fr/memphis/

Institut de Mathématiques de Bordeaux

informatics mathematics

Re-use simulations for parametric modeling

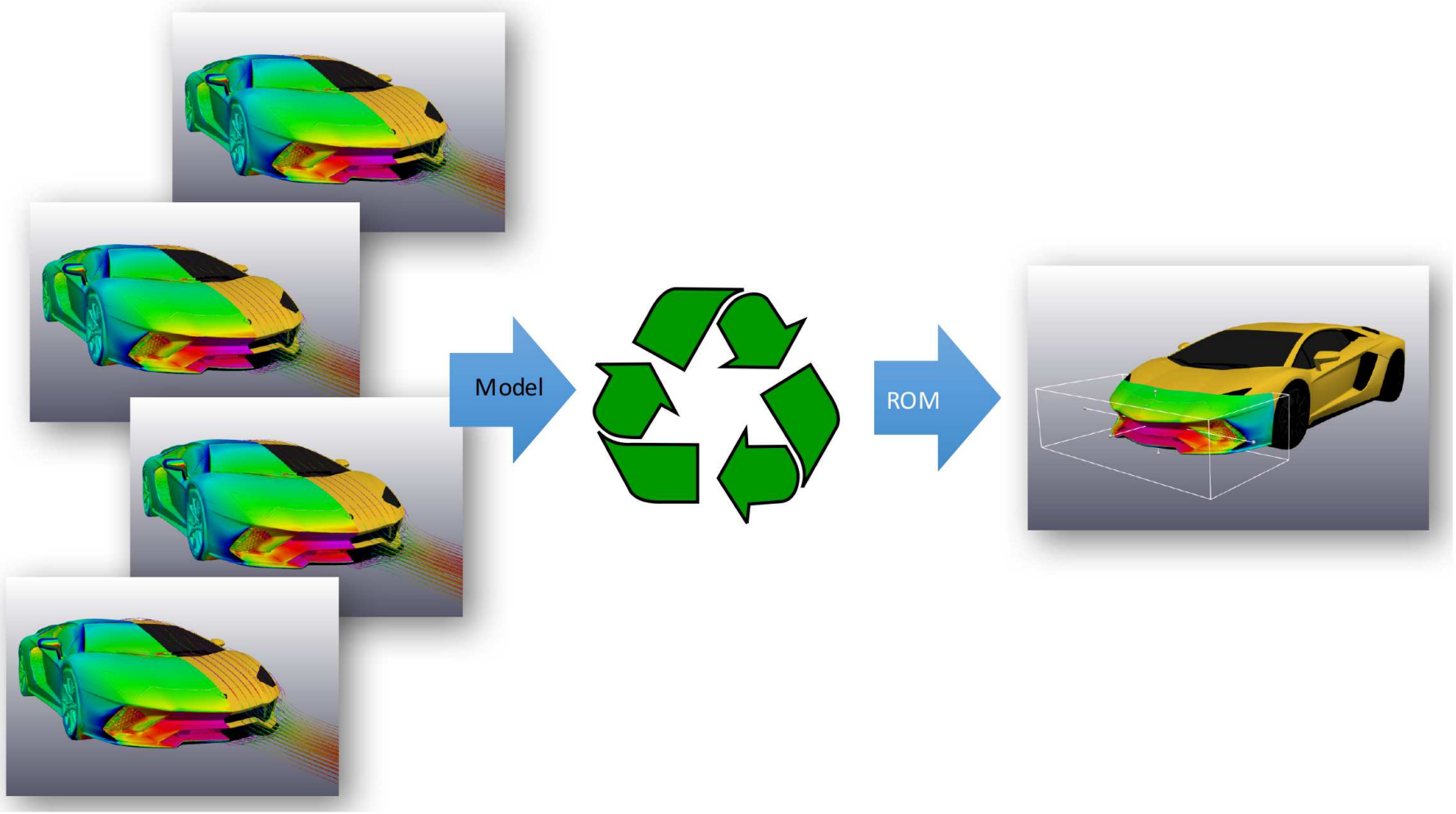

Toy problem: superposition principle

Elastic membrane defined in $\Omega \subset \mathbb{R}^2$ with compact support loads $f_i \in L^2(\Omega)$, e.g., bump functions:

$$f_i = e^{-\frac{1}{(\epsilon^2-(x-x_i)^2)}} \mathbb{1}_{|x-x_i|<\epsilon}$$

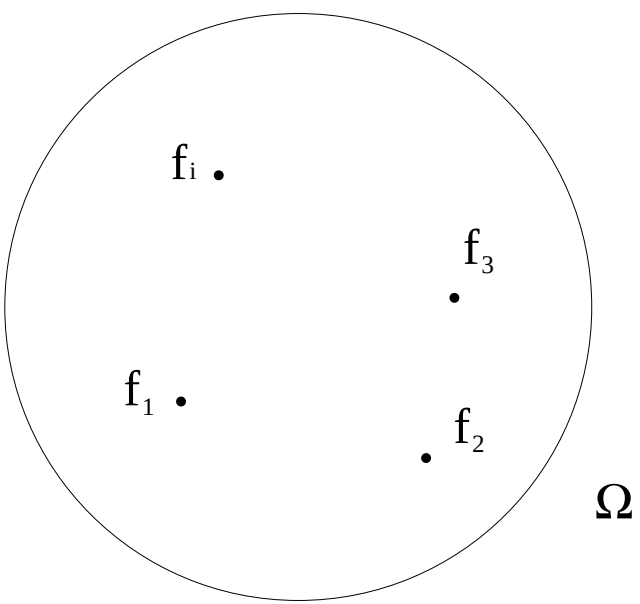

Toy problem: superposition principle

Elastic membrane defined in $\Omega \subset \mathbb{R}^2$ with compact support loads $f_i \in L^2(\Omega)$, e.g., bump functions:

$$f_i = e^{-\frac{1}{(\epsilon^2-(x-x_i)^2)}} \mathbb{1}_{|x-x_i|<\epsilon}$$

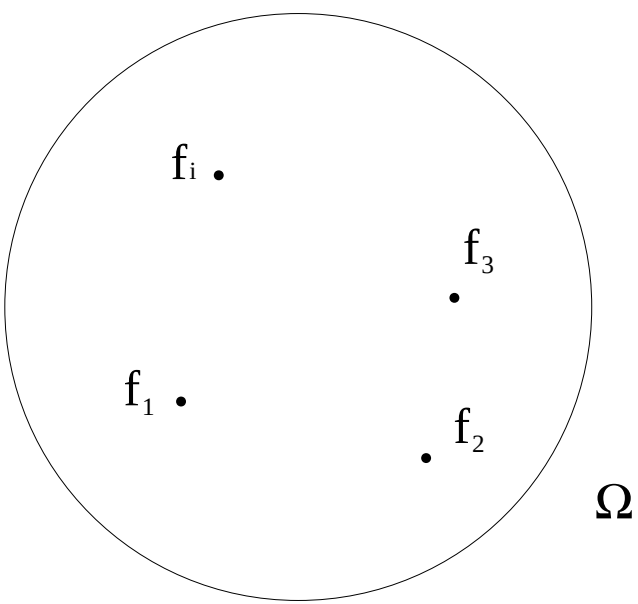

The classical model is

$$-\Delta u = f = f_0 + \alpha_1 f_1 + \alpha_2 f_2 + \dots$$

with $i = 1, \cdots, N$, $u|_{\partial\Omega} = 0$ and where the coefficients $\alpha_i \in \mathbb{R}$ model the intensity of the load in x_i.

Institut de Mathématiques de Bordeaux

informatics mathematics Inria

Toy problem: superposition principle

Elastic membrane defined in $\Omega \subset \mathbb{R}^2$ with compact support loads $f_i \in L^2(\Omega)$, e.g., bump functions:

$$f_i = e^{-\frac{1}{(\epsilon^2-(x-x_i)^2)}} \mathbb{1}_{|x-x_i|<\epsilon}$$

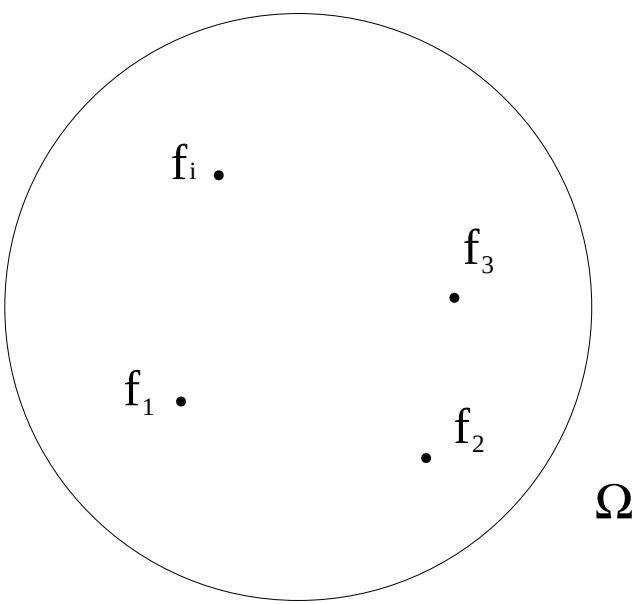

The classical model is

$$-\Delta u = f = f_0 + \alpha_1 f_1 + \alpha_2 f_2 + \dots$$

with $i = 1, \cdots, N$, $u|_{\partial\Omega} = 0$ and where the coefficients $\alpha_i \in \mathbb{R}$ model the intensity of the load in x_i.

The solution is of course

$$u = u_0 + \alpha_1 u_1 + \alpha_2 u_2 + \cdots$$

where $-\Delta u_i = f_i$ and $u_i|_{\partial\Omega} = 0$

Institut de Mathématiques de Bordeaux

informatics mathematics Inria

Offline - Online paradigm

We want to solve $-\Delta u = f$, $u|_{\partial\Omega} = 0$

Offline step

Offline - Online paradigm

We want to solve $-\Delta u = f$, $u|_{\partial\Omega} = 0$

Offline step

Sampling in parameter space: solve for $i = 1, \cdots, N$

$$-\Delta u_i = f_i \text{ with } u_i|_{\partial\Omega} = 0$$

Institut de Mathématiques de Bordeaux

informatics mathematics

Offline - Online paradigm

We want to solve $-\Delta u = f$, $u|_{\partial\Omega} = 0$

Offline step

Sampling in parameter space: solve for $i = 1, \cdots, N$

$$-\Delta u_i = f_i \text{ with } u_i|_{\partial\Omega} = 0$$

Approximation space

$$V = \text{Span}\{u_1, \cdots, u_N\}$$

Institut de Mathématiques de Bordeaux

informatics mathematics

Offline - Online paradigm

We want to solve $-\Delta u = f$, $u|_{\partial\Omega} = 0$

Offline step

Sampling in parameter space: solve for $i = 1, \cdots, N$

$$-\Delta u_i = f_i \text{ with } u_i|_{\partial\Omega} = 0$$

Approximation space

$$V = \text{Span}\{u_1, \cdots, u_N\}$$

Online step

Offline - Online paradigm

We want to solve $-\Delta u = f$, $u|_{\partial\Omega} = 0$

Offline step

Sampling in parameter space: solve for $i = 1, \cdots, N$

$$-\Delta u_i = f_i \text{ with } u_i|_{\partial\Omega} = 0$$

Approximation space

$$V = \text{Span}\{u_1, \cdots, u_N\}$$

Online step

If the load configuration is fixed, then $f = \sum_i \alpha_i f_i \in W = \text{Span}\{f_1, \cdots, f_N\}$ and hence $u \in V$

Offline - Online paradigm

We want to solve $-\Delta u = f$, $u|_{\partial\Omega} = 0$

Offline step

Sampling in parameter space: solve for $i = 1, \cdots, N$

$$-\Delta u_i = f_i \text{ with } u_i|_{\partial\Omega} = 0$$

Approximation space

$$V = \text{Span}\{u_1, \cdots, u_N\}$$

Online step

If the load configuration is fixed, then $f = \sum_i \alpha_i f_i \in W = \text{Span}\{f_1, \cdots, f_N\}$ and hence $u \in V$

Linear interpolation in V: $u = \sum_i \alpha_i u_i$

Offline - Online paradigm

We want to solve $-\Delta u = f$, $u|_{\partial\Omega} = 0$

Offline step

Sampling in parameter space: solve for $i = 1, \cdots, N$

$$-\Delta u_i = f_i \text{ with } u_i|_{\partial\Omega} = 0$$

Approximation space

$$V = \text{Span}\{u_1, \cdots, u_N\}$$

Online step

If the load configuration is fixed, then $f = \sum_i \alpha_i f_i \in W = \text{Span}\{f_1, \cdots, f_N\}$ and hence $u \in V$

Linear interpolation in V: $u = \sum_i \alpha_i u_i$

PDE approach $\Rightarrow \min_{\alpha_i} \mathcal{R}(\alpha_i)$, $\quad \mathcal{R}(\alpha_i) = \|\Delta u + f\|$: N is possibly small !

Institut de Mathématiques de Bordeaux

informatics mathematics

Sampling and interpolation

For arbitrary f, we may have (compact support loads):

$$proj_W(f) = 0 \text{ and therefore } u = 0 \text{ in } V$$

Institut de Mathématiques de Bordeaux

informatics mathematics

Sampling and interpolation

For arbitrary f, we may have (compact support loads):

$$proj_W(f) = 0 \text{ and therefore } u = 0 \text{ in } V$$

$\Rightarrow$ Optimal sampling of the parameter space

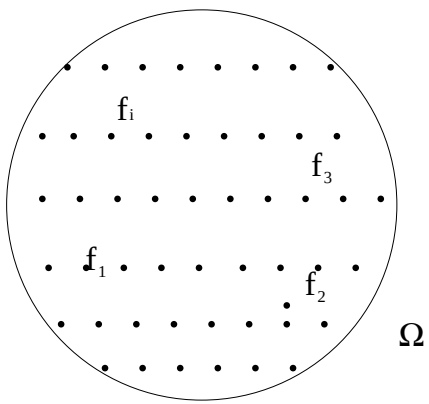

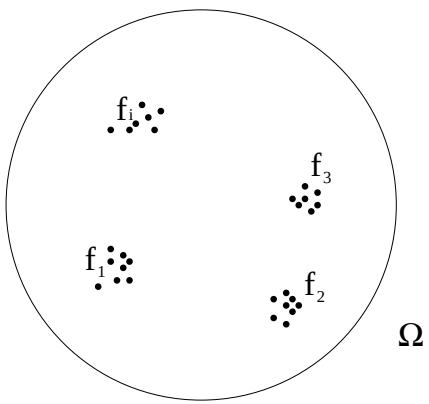

Sampling and interpolation

For arbitrary f, we may have (compact support loads):

$$proj_W(f) = 0 \text{ and therefore } u = 0 \text{ in } V$$

$\Rightarrow$ Optimal sampling of the parameter space

$\Rightarrow$ Interpolate the approximation space

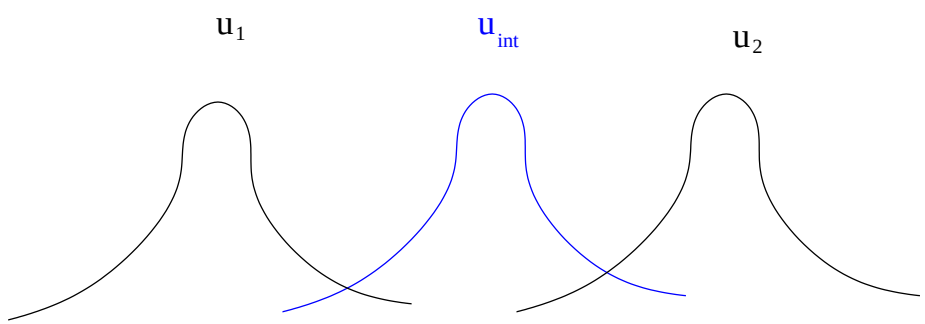

Approximation subspace and data compression (POD)

Data and Model I

Approximation subspace and data compression (POD)

Data and Model I

Subspace interpolation

Approximation subspace and data compression (POD)

Data and Model I

Subspace interpolation

Low-fidelity samples: Monge problem

Institut de Mathématiques de Bordeaux

informatics mathematics

Approximation subspace and data compression (POD)

Data and Model I

Subspace interpolation

Low-fidelity samples: Monge problem

Application to BGK equation

Approximation subspace and data compression (POD)

- Data and Model I
  - Subspace interpolation
  - Low-fidelity samples: Monge problem
  - Application to BGK equation
- Data and Model II

Institut de Mathématiques de Bordeaux

informatics mathematics

Approximation subspace and data compression (POD)

- Data and Model I
  - Subspace interpolation
  - Low-fidelity samples: Monge problem
  - Application to BGK equation
- Data and Model II
  - FOM/ROM Coupling

Institut de Mathématiques de Bordeaux

informatics mathematics

Approximation subspace and data compression (POD)

- Data and Model I
  - Subspace interpolation
  - Low-fidelity samples: Monge problem
  - Application to BGK equation
- Data and Model II
  - FOM/ROM Coupling
  - Convergence between data and simulation: an industrial case

Institut de Mathématiques de Bordeaux

informatics mathematics

Approximation subspace and data compression (POD)

- Data and Model I
  - Subspace interpolation
  - Low-fidelity samples: Monge problem
  - Application to BGK equation
- Data and Model II
  - FOM/ROM Coupling
  - Convergence between data and simulation: an industrial case
- Perspectives

Institut de Mathématiques de Bordeaux

informatics mathematics

Approximation subspace

Data compression

Proper Orthogonal Decomposition (POD), Lumley (1967)

▷ Define a subspace $V = \text{Span}\{\boldsymbol{\Phi}\}$ where the projection of the samples $\boldsymbol{u}$ is optimal.

▷ $\boldsymbol{\Phi}$ is given by

$$\boldsymbol{\Phi} = \arg\max_{\boldsymbol{\Psi}} \langle |(\boldsymbol{u}, \boldsymbol{\Psi})|^2 \rangle, \quad \|\boldsymbol{\Phi}\|^2 = 1.$$

▷ Eckart–Young–Mirsky theorem:

$$RIC(M) = \sum_{k=1}^{p} \lambda_k \Big/ \sum_{k=1}^{n_s} \lambda_k$$

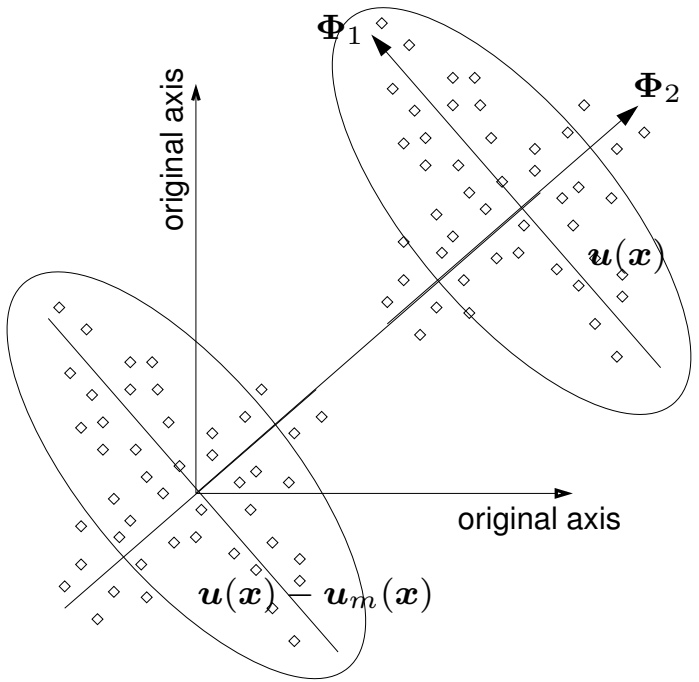

Lumley J.L. (1967) : The structure of inhomogeneous turbulence. *Atmospheric Turbulence and Wave Propagation*, ed. A.M. Yaglom & V.I. Tatarski, pp. 166-178.

Data compression

Example: 2D cylinder wake flow $Re = 200$ for $\boldsymbol{u} = (\boldsymbol{U},\ P)^T$ with $n_s = 200$

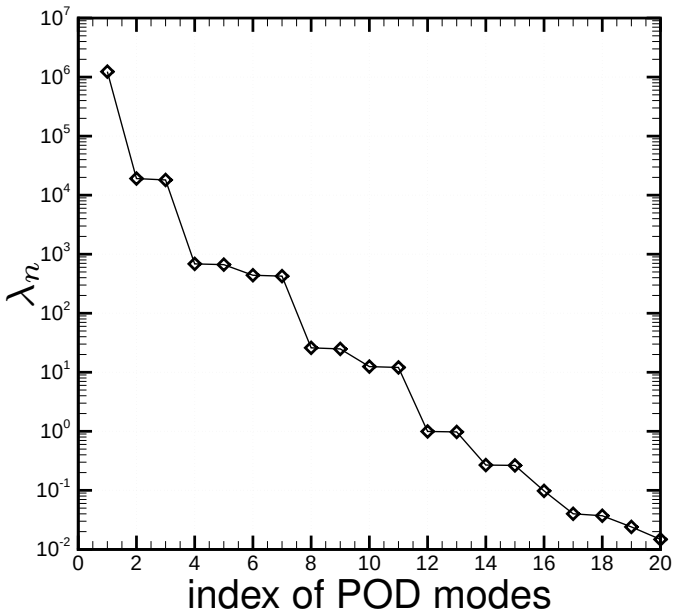

Fig. : *POD spectrum.*

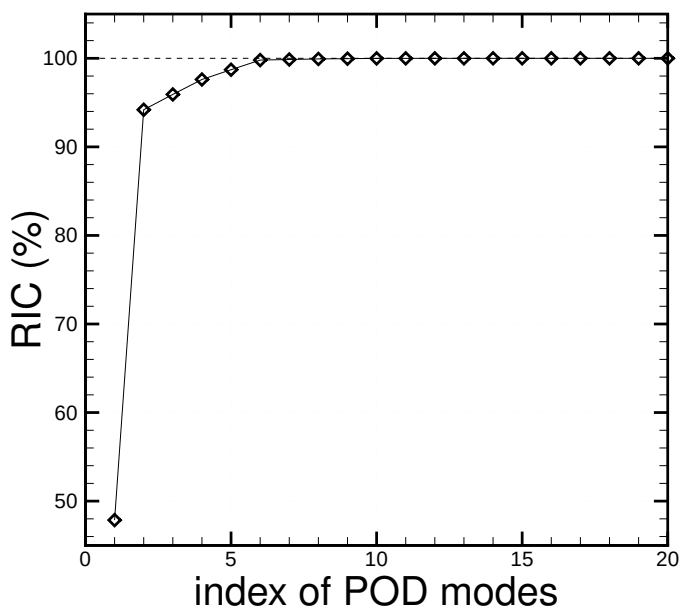

Fig. : *RIC(p), p nb POD modes.*

Subspace interpolation

Subspace interpolation: geodesics

Let $V_{n,p} = \left\{ \Gamma \in \mathcal{M}_{n,p}(\mathbb{R}); \Gamma^T \Gamma = I, p \leq n \right\}$

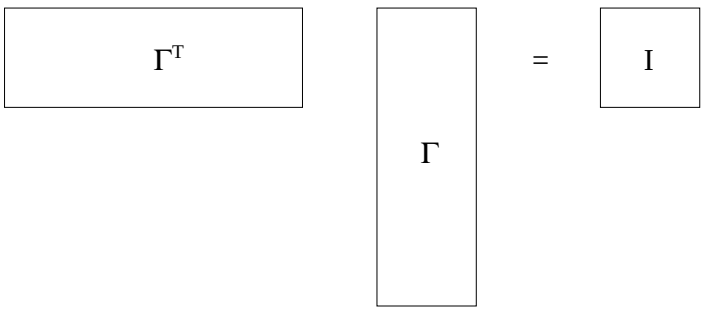

Scalar product in $V_{n,p}$: $< \Gamma_1, \Gamma_2 > =$ Trace $\left(\Gamma_1^T \Gamma_2 \right)$

D. Amsallem and C. Farhat. "Interpolation Method for Adapting Reduced-Order Models and Application to Aeroelasticity", AIAA Journal, Vol. 46, No. 7 (2008), pp. 1803-1813.

Institut de Mathématiques de Bordeaux

informatics mathematics Inria

Subspace interpolation: geodesics

Let $V_{n,p} = \left\{ \Gamma \in \mathcal{M}_{n,p}(\mathbb{R}); \Gamma^T \Gamma = I, p \leq n \right\}$

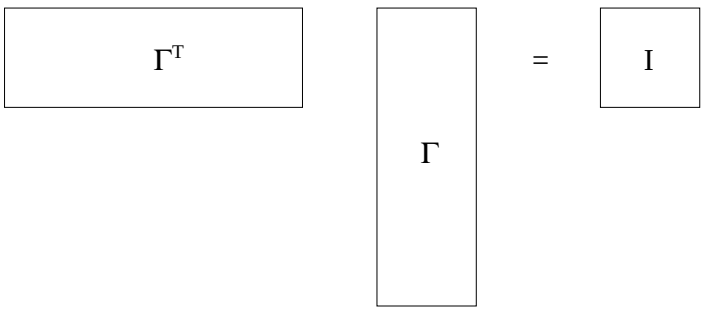

Scalar product in $V_{n,p}$: $< \Gamma_1, \Gamma_2 > =$ Trace $\left(\Gamma_1^T \Gamma_2 \right)$

Consider the projections $\mathcal{P}_1 = \Gamma_1 \Gamma_1^T$ and $\mathcal{P}_2 = \Gamma_2 \Gamma_2^T$

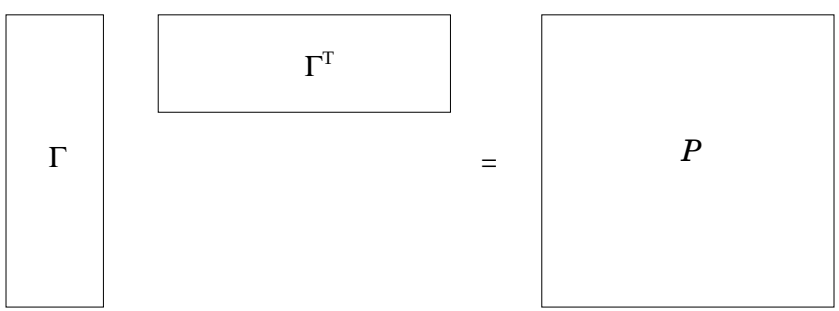

If $\mathcal{P}_1 = \mathcal{P}_2$, then $\Gamma_1 \sim \Gamma_2$: they represent the same element in the set of p-dimensional subspaces in $\mathbb{R}^n$, $G_{n,p}$

D. Amsallem and C. Farhat. "Interpolation Method for Adapting Reduced-Order Models and Application to Aeroelasticity", AIAA Journal, Vol. 46, No. 7 (2008), pp. 1803-1813.

Institut de Mathématiques de Bordeaux

informatics mathematics Inria

Subspace interpolation: geodesics

Let now $\Gamma(t) : [0, 1] \to V_{n,p}$ be a function of a scalar parameter t

Subspace interpolation: geodesics

Let now $\Gamma(t) : [0, 1] \to V_{n,p}$ be a function of a scalar parameter t

A geodesic in $G_{n,p}$ satisfies the contraint $\dot{\Gamma}^T \Gamma = 0$ and the normal acceleration equation $< \dot{\Gamma}, \ddot{\Gamma} > = 0$.

Institut de Mathématiques de Bordeaux

informatics mathematics

Subspace interpolation: geodesics

Let now $\Gamma(t) : [0, 1] \to V_{n,p}$ be a function of a scalar parameter t

A geodesic in $G_{n,p}$ satisfies the contraint $\dot{\Gamma}^T \Gamma = 0$ and the normal acceleration equation $< \dot{\Gamma}, \ddot{\Gamma} > = 0$.

Combining these equations:

$$\ddot{\Gamma} + \Gamma H = 0$$

where $H \in \mathcal{S}_p(\mathbb{R})$, $H = \dot{\Gamma}^T \dot{\Gamma}$, $\dot{H} = 0$

Institut de Mathématiques de Bordeaux

informatics mathematics

Subspace interpolation: geodesics

Let now $\Gamma(t) : [0, 1] \to V_{n,p}$ be a function of a scalar parameter t

A geodesic in $G_{n,p}$ satisfies the contraint $\dot{\Gamma}^T \Gamma = 0$ and the normal acceleration equation $< \dot{\Gamma}, \ddot{\Gamma} > = 0$.

Combining these equations:

$$\ddot{\Gamma} + \Gamma H = 0$$

where $H \in \mathcal{S}_p(\mathbb{R})$, $H = \dot{\Gamma}^T \dot{\Gamma}$, $\dot{H} = 0$

This equation encodes the notion of 0 acceleration in the tangent space and the fact that Γ and $\Gamma + d\Gamma$ have different projections, i.e., $< \Gamma, d\Gamma > = 0$

Institut de Mathématiques de Bordeaux

informatics mathematics

Subspace interpolation: geodesics

Let now $\Gamma(t) : [0, 1] \to V_{n,p}$ be a function of a scalar parameter t

A geodesic in $G_{n,p}$ satisfies the contraint $\dot{\Gamma}^T \Gamma = 0$ and the normal acceleration equation $< \dot{\Gamma}, \ddot{\Gamma} > = 0$.

Combining these equations:

$$\ddot{\Gamma} + \Gamma H = 0$$

where $H \in \mathcal{S}_p(\mathbb{R})$, $H = \dot{\Gamma}^T \dot{\Gamma}$, $\dot{H} = 0$

This equation encodes the notion of 0 acceleration in the tangent space and the fact that Γ and $\Gamma + d\Gamma$ have different projections, i.e., $< \Gamma, d\Gamma > = 0$

We have:

$$\Gamma(t) = \Gamma_0 \, v \cos(\Sigma t) + u \sin(\Sigma t)$$

where $\Gamma_0 = \Gamma(0)$, $\dot{\Gamma}_0 = \dot{\Gamma}(0) = u \, \Sigma \, v^T$. Thin svd: $u \in \mathcal{M}_{n,p}(\mathbb{R})$, $u^T u = I$, $v \in \mathcal{M}_{p,p}(\mathbb{R})$, $v^T v = I$, $\Sigma \in \text{diag}_p(\mathbb{R})$

Application to sampling

Geodesic distance example

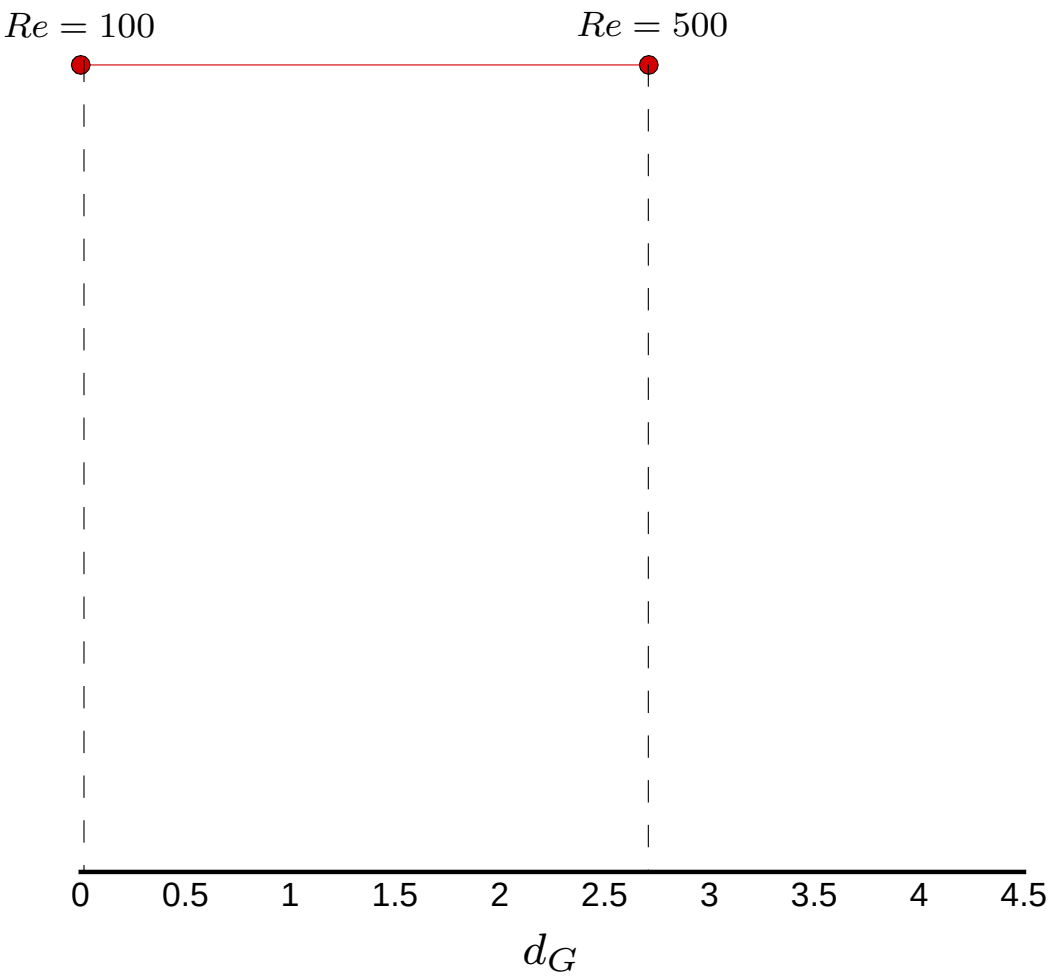

Initial sampling with $Re = 100$ *and* $Re = 500$
50 snapshots on one vortex shedding period, 7 modes

Institut de Mathématiques de Bordeaux

informatics mathematics

Geodesic distance example

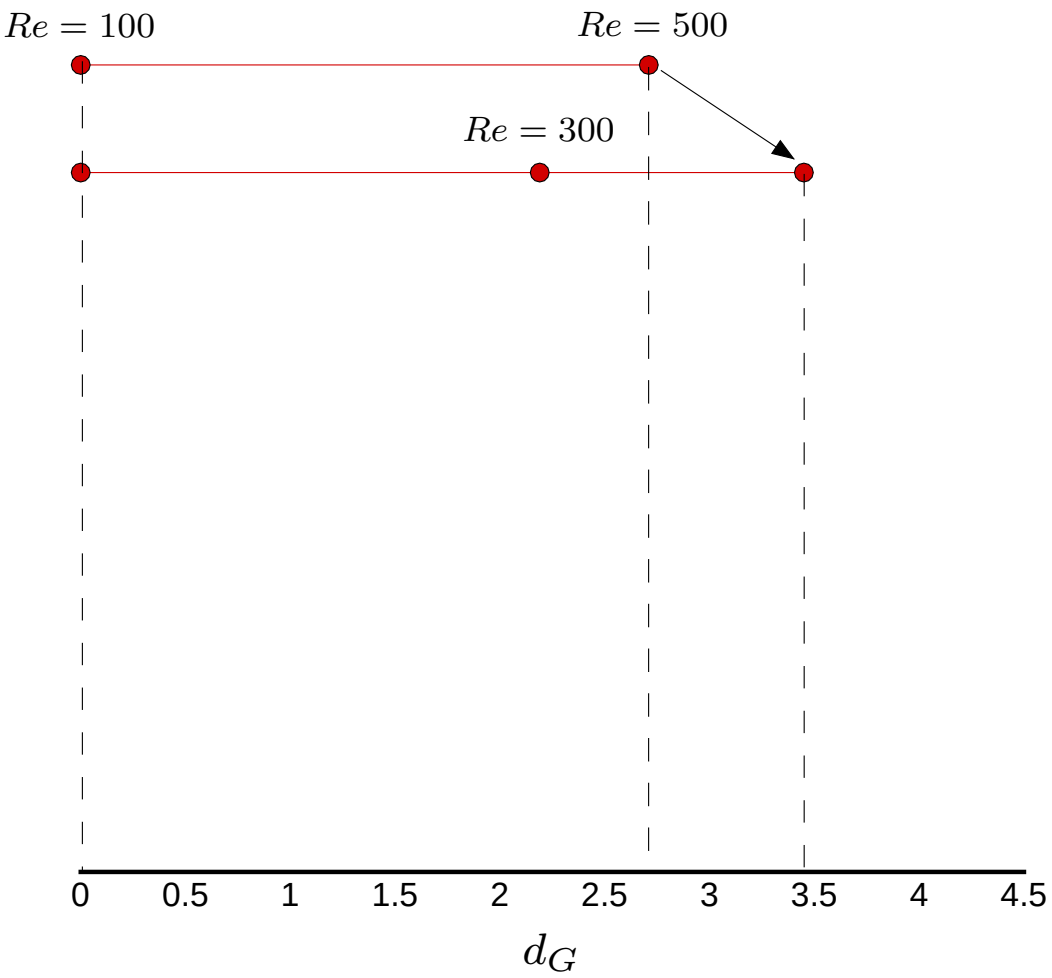

$Re = 300$ *is not on the geodesic between* $Re = 100 \leftrightarrow Re = 500$

Geodesic distance example

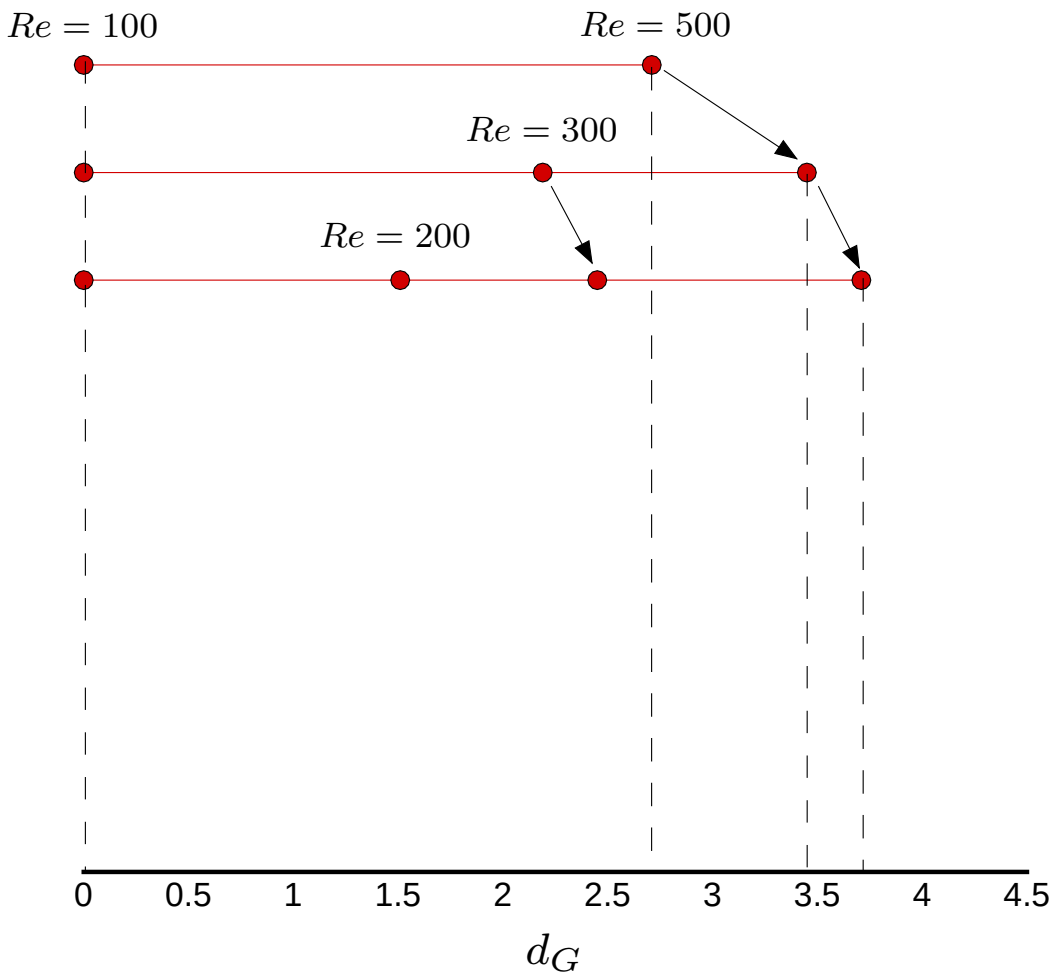

$Re = 200$ *is not on the geodesic* $Re = 100 \leftrightarrow Re = 300$

Geodesic distance example

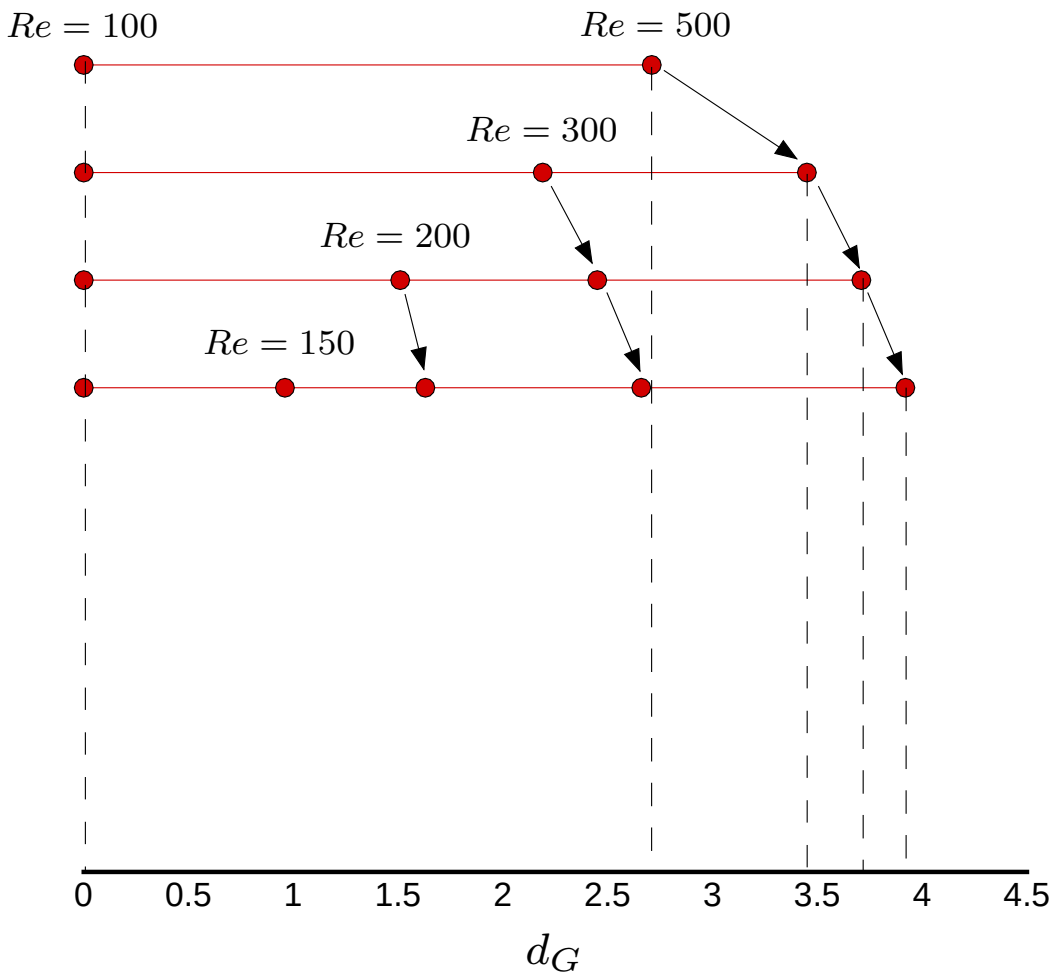

$Re = 150$ *is not on the geodesic* $Re = 100 \leftrightarrow Re = 200$

Geodesic distance example

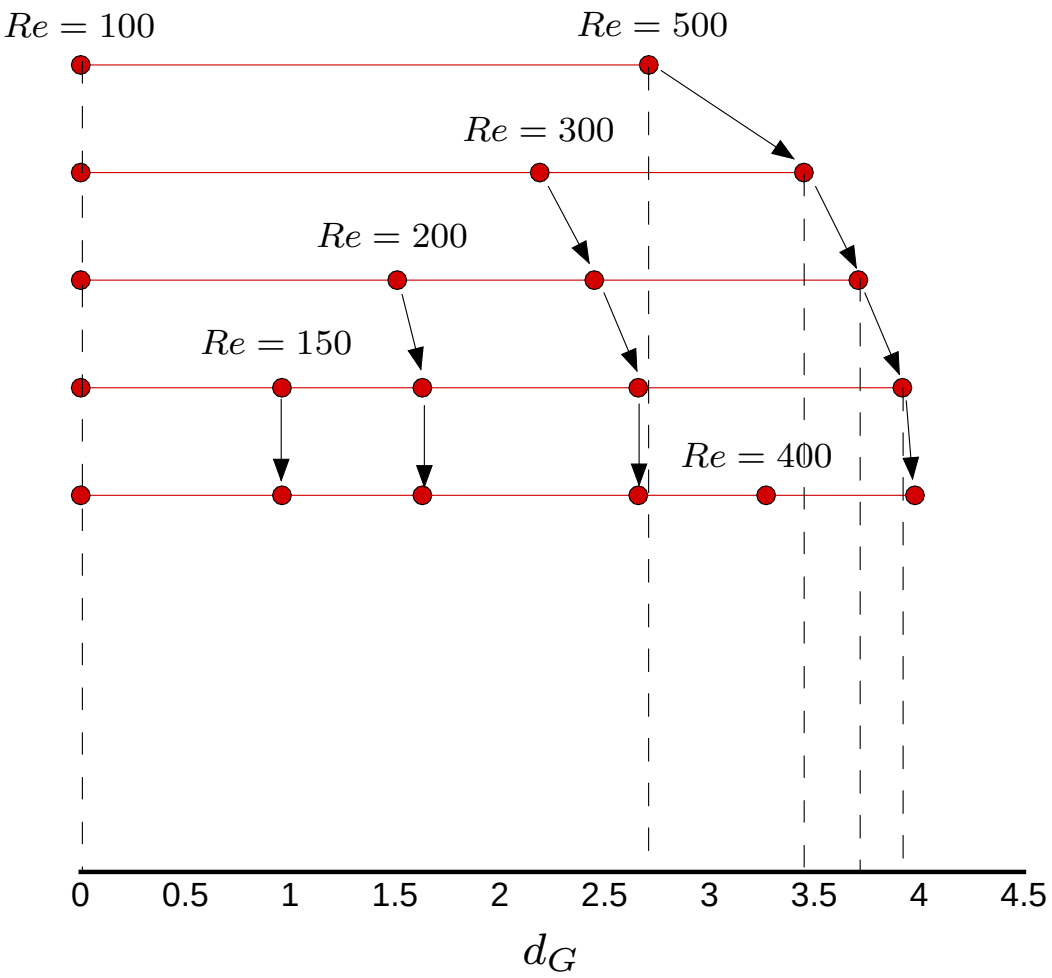

$Re = 400$ *is almost on the geodesic* $Re = 300 \leftrightarrow Re = 500$

Geodesic distance example

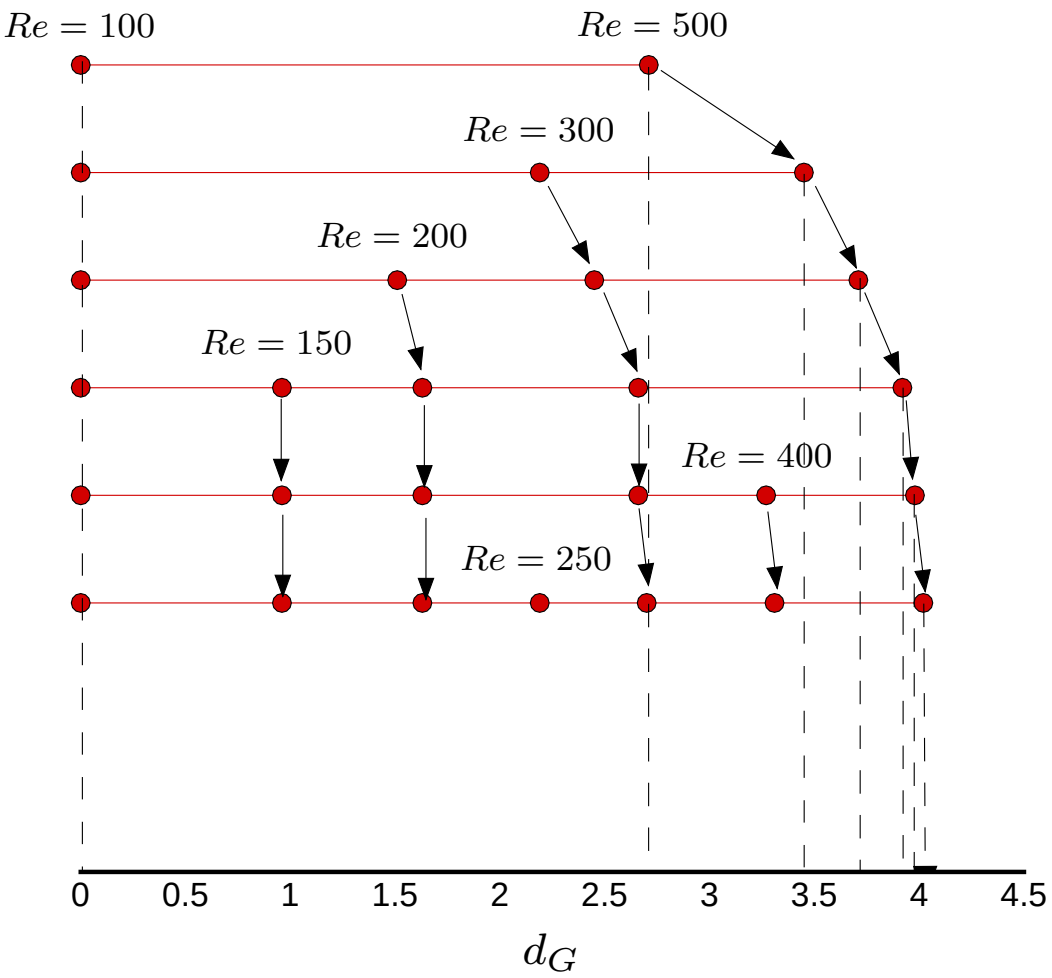

$Re = 250$ *is almost on the geodesic* $Re = 200 \leftrightarrow Re = 300$

Geodesic distance example

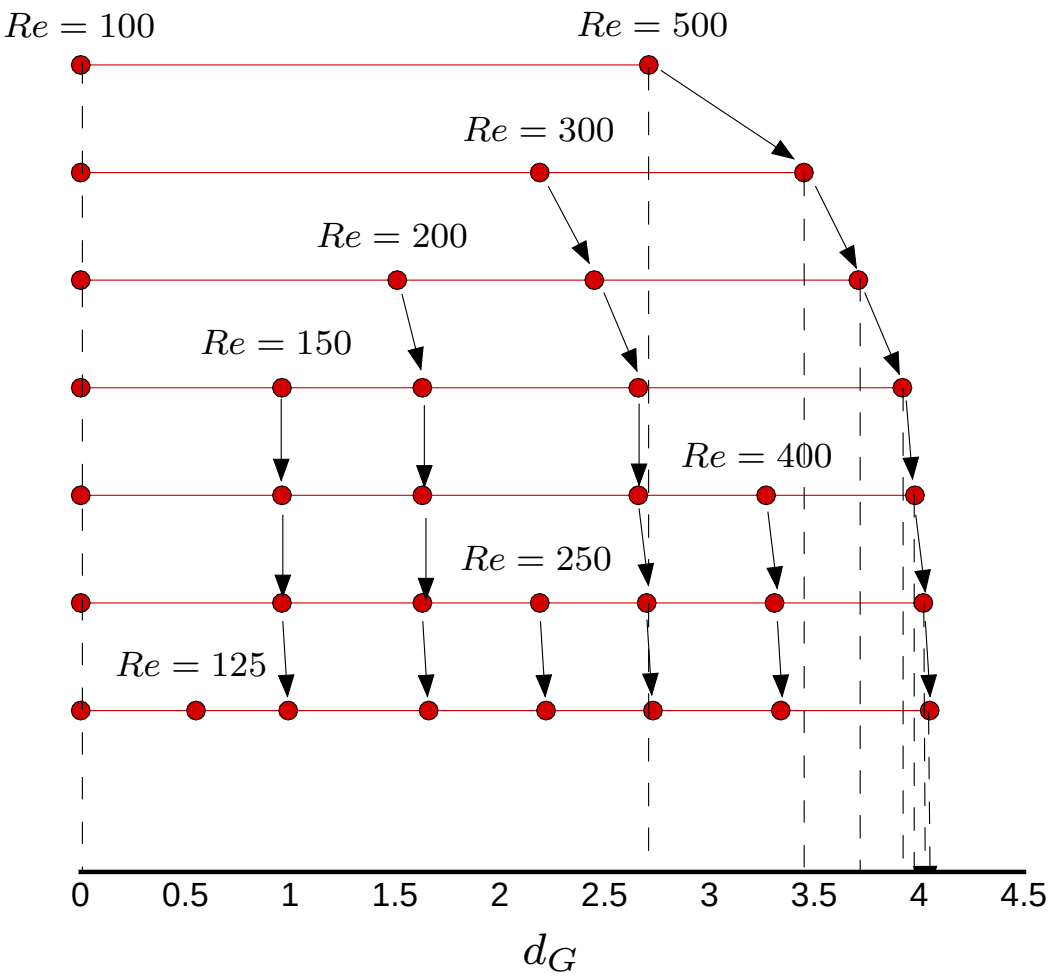

$Re = 125$ *is almost on the geodesic* $Re = 100 \leftrightarrow Re = 150$

Geodesic distance example

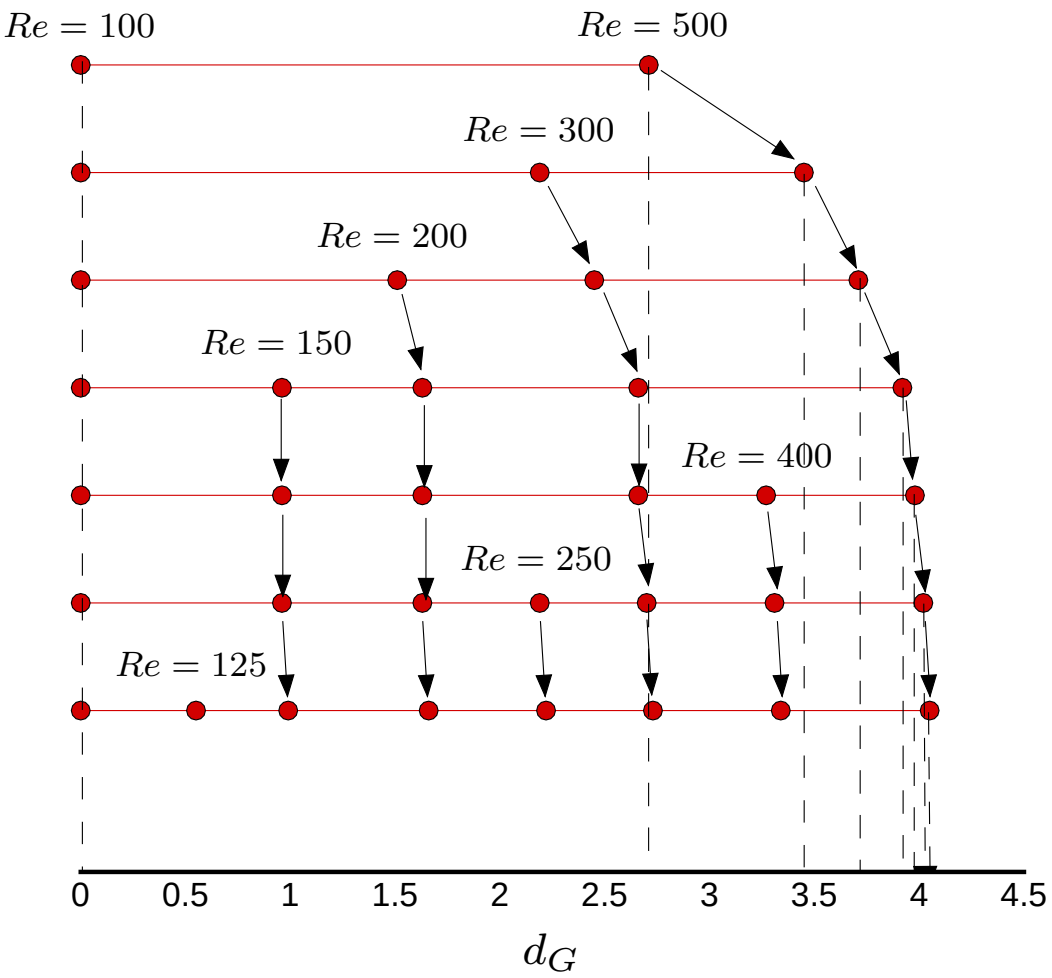

$Re = 125$ *is almost on the geodesic* $Re = 100 \leftrightarrow Re = 150$

Almost uniform sampling in the solution space

Geodesic interpolation: 1D advection

We have two sets of solution samples S_1, S_2 shifted of $7\delta x$, from which we determine $\Gamma_1, \Gamma_2 \in V_{201,2}(\mathbb{R})$

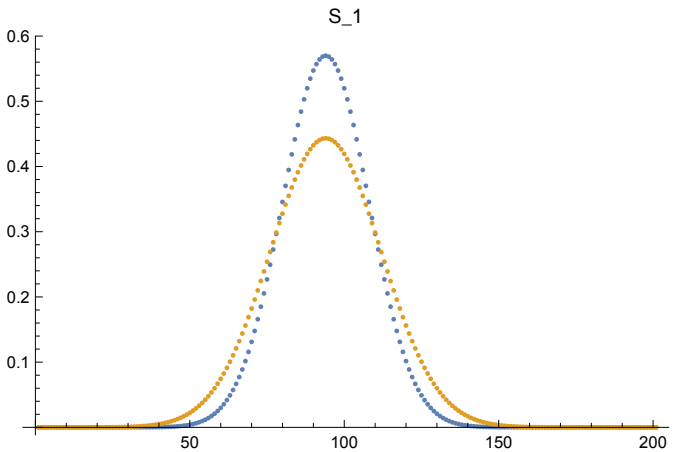

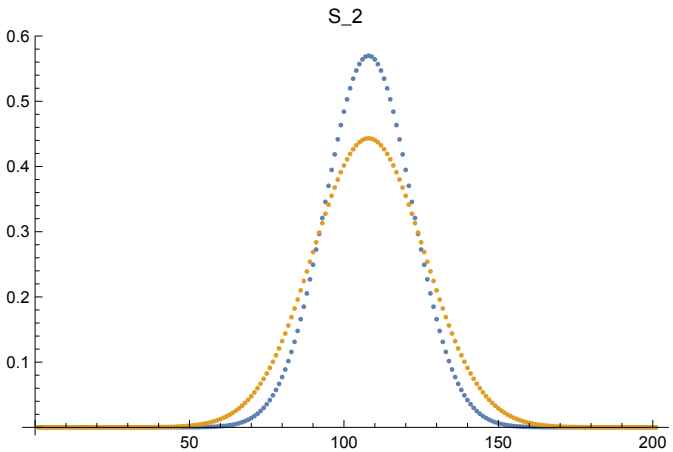

Institut de Mathématiques de Bordeaux

informatics mathematics

Geodesic interpolation: 1D advection

We have two sets of solution samples S_1, S_2 shifted of $7\delta x$, from which we determine $\Gamma_1, \Gamma_2 \in V_{201,2}(\mathbb{R})$

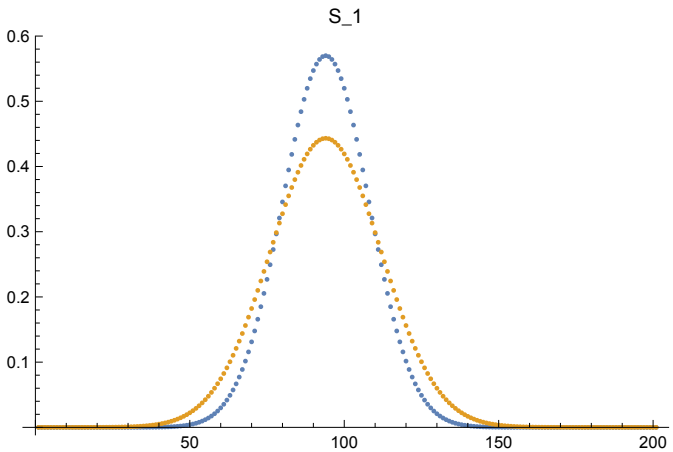

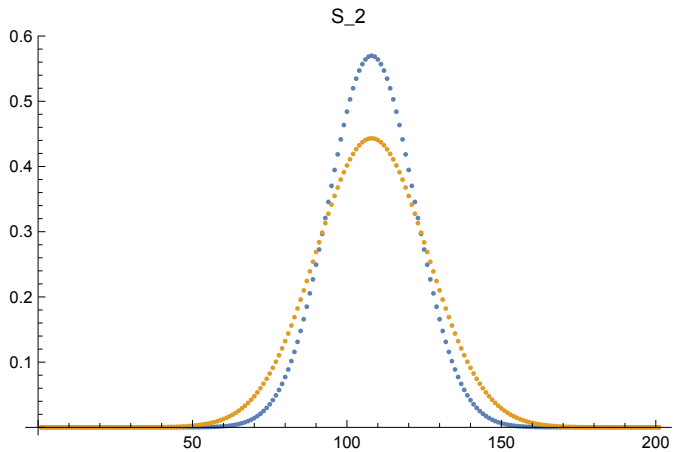

The maximum distance in temrs of principal angles is almost $\frac{\pi}{2}$

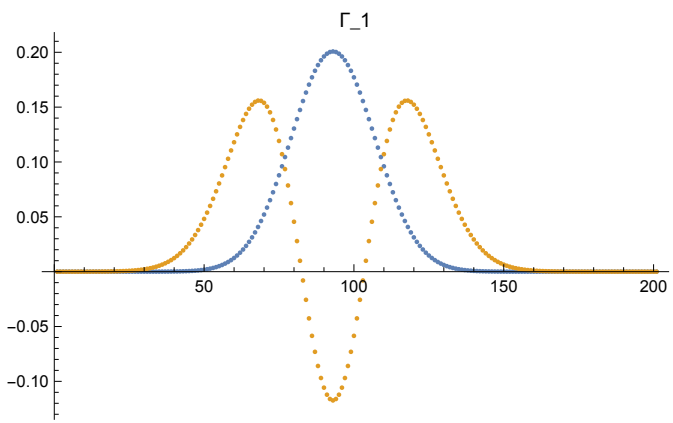

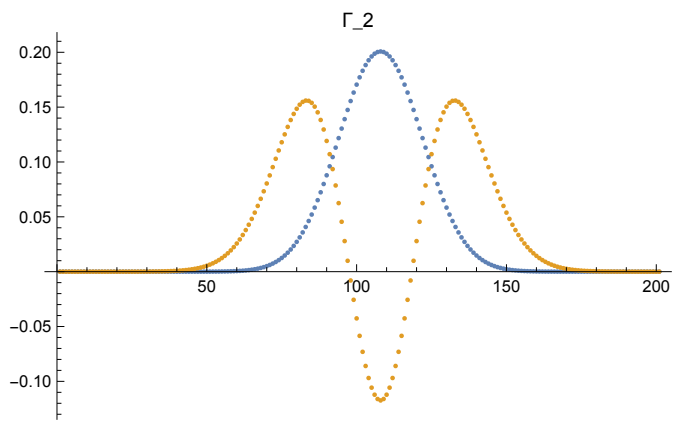

Institut de Mathématiques de Bordeaux

informatics mathematics

Geodesic interpolation: 1D advection

Shifted of $7\,\delta x$: expected Γ_1 and Γ_2 and projection on interpolated subspace

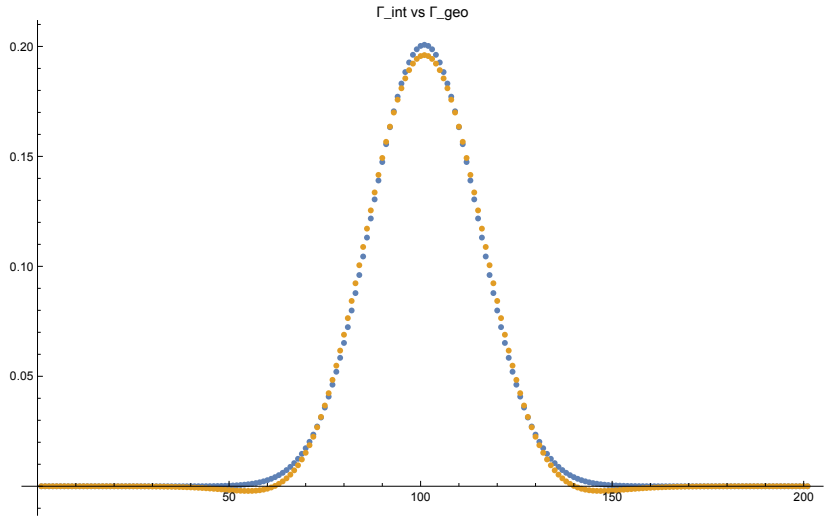

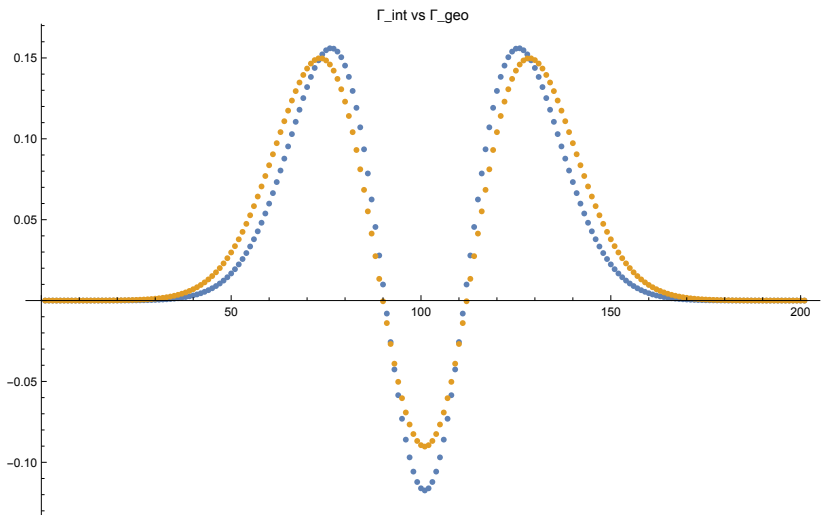

Institut de Mathématiques de Bordeaux

informatics mathematics Inria

Geodesic interpolation: 1D advection

Shifted of $7\,\delta x$: expected Γ_1 and Γ_2 and projection on interpolated subspace

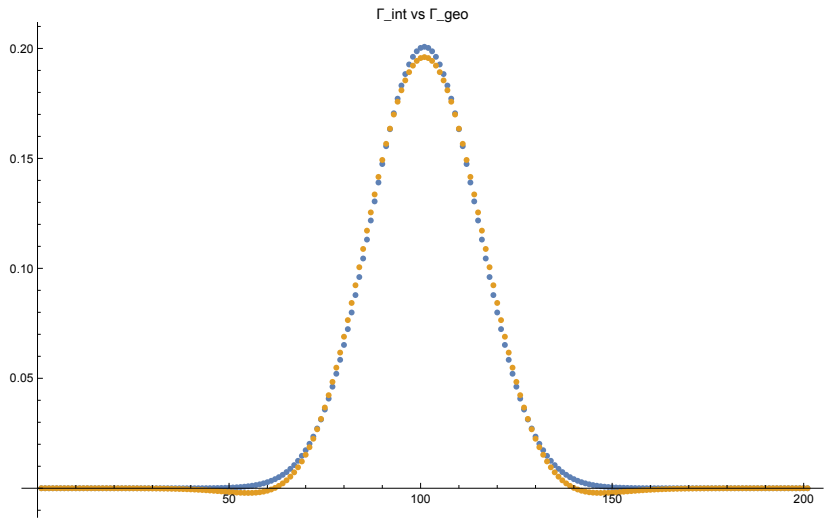

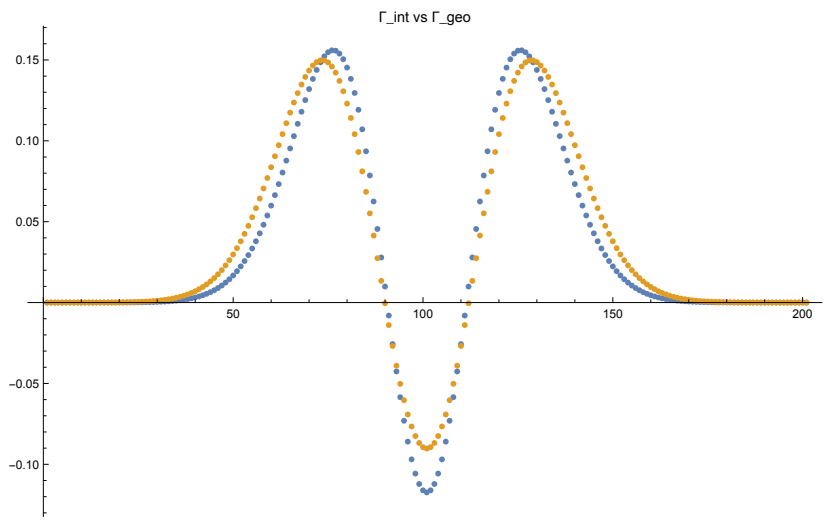

Shift of $8\,\delta x$: one of the principal angles crosses $\dfrac{\pi}{2}$

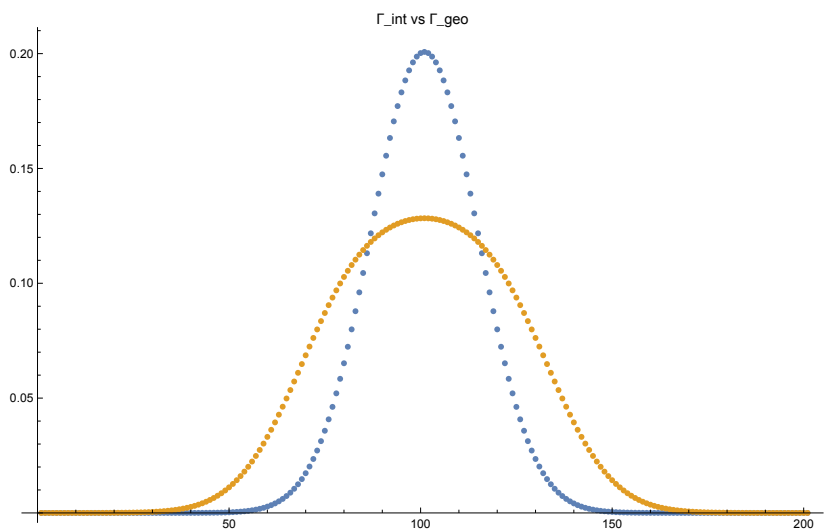

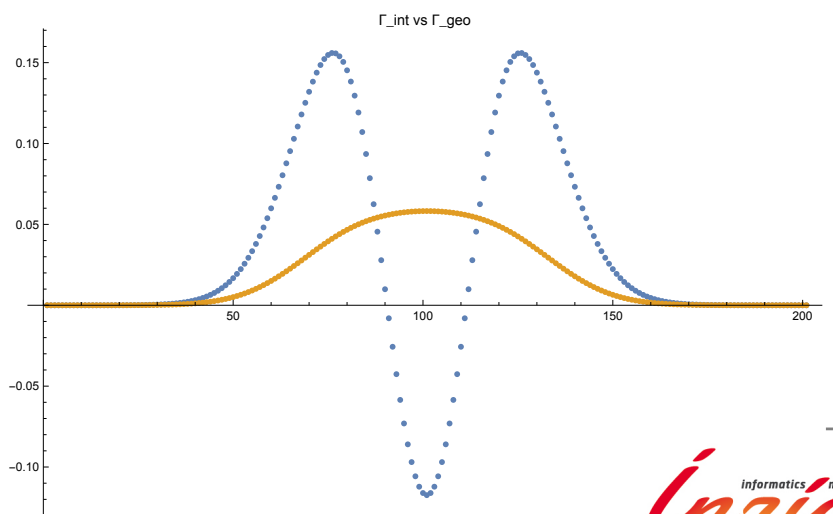

Institut de Mathématiques de Bordeaux

informatics mathematics

McCann's interpolation

Geodesic interpolation: Wasserstein distance

Given two unit densities $\rho_0(\xi)$ and $\rho_1(x)$ in $\mathbb{R}^d$, the Monge problem (Théorie des Déblais & des Remblais, 1781 or the Monge barrow) of optimal transportation defines a distance:

Institut de Mathématiques de Bordeaux

informatics mathematics

Geodesic interpolation: Wasserstein distance

Given two unit densities $\rho_0(\xi)$ and $\rho_1(x)$ in $\mathbb{R}^d$, the Monge problem (Théorie des Déblais & des Remblais, 1781 or the Monge barrow) of optimal transportation defines a distance:

$$d^2(\rho_1, \rho_0) = \inf_X \int_{\mathbb{R}^d} \rho_0(\xi)\,(X(\xi) - \xi)^2\, d\xi$$

subject to mass conservation:

$$\rho_0(\xi) = \rho_1(X(\xi))\det(\nabla X(\xi))$$

Geodesic interpolation: Wasserstein distance

Given two unit densities $\rho_0(\xi)$ and $\rho_1(x)$ in $\mathbb{R}^d$, the Monge problem (Théorie des Déblais & des Remblais, 1781 or the Monge barrow) of optimal transportation defines a distance:

$$d^2(\rho_1, \rho_0) = \inf_X \int_{\mathbb{R}^d} \rho_0(\xi)\,(X(\xi) - \xi)^2\, d\xi$$

subject to mass conservation:

$$\rho_0(\xi) = \rho_1(X(\xi))\det(\nabla X(\xi))$$

Let $X^*(\xi)$ the optimal map, the geodesic map $\gamma(t) = (1-t)\,\xi + t\,X^*(\xi)$, $0 \le t \le 1$ defines a set of interpolated densities

Institut de Mathématiques de Bordeaux

informatics mathematics

Geodesic interpolation: Wasserstein distance

Given two unit densities $\rho_0(\xi)$ and $\rho_1(x)$ in $\mathbb{R}^d$, the Monge problem (Théorie des Déblais & des Remblais, 1781 or the Monge barrow) of optimal transportation defines a distance:

$$d^2(\rho_1, \rho_0) = \inf_X \int_{\mathbb{R}^d} \rho_0(\xi)\,(X(\xi) - \xi)^2\, d\xi$$

subject to mass conservation:

$$\rho_0(\xi) = \rho_1(X(\xi))\det(\nabla X(\xi))$$

Let $X^*(\xi)$ the optimal map, the geodesic map $\gamma(t) = (1-t)\,\xi + t\,X^*(\xi)$, $0 \leq t \leq 1$ defines a set of interpolated densities

Existence and unicity of the solution but diffucult to find without (entropy) regularization $\Rightarrow$ Kullback-Leibler divegrence.

Convolutional Wasserstein Distances: Efficient Optimal Transportation on Geometric Domains. J.Solomon, A. Butscher, F. de Goes, A. Nguyen. G. Peyré, M. Cuturi, T. Du, L. Guibas. ACM Transactions on Graphics (Proc. SIGGRAPH 2015), 34(4), 2015.

Institut de Mathématiques de Bordeaux

informatics mathematics Inria

BB continuum mechanics formulation

Action minimization

$$\inf_{\rho,u} \int_{\mathbb{R}^d \times [0,1]} \frac{\rho\, u^2}{2}\, dx\, dt$$

subject to mass conservation. The resulting Euler-Lagrange equations are:

$$\partial_t \rho + \nabla \cdot (\rho u) = 0$$

$$\partial_t u + u \cdot \nabla u = 0$$

$$\rho(x, t = 0) = \rho_0(x) \text{ and } \rho(x, t = 1) = \rho_1(x)$$

$$u = \nabla \phi$$

where ϕ is the Lagrange multiplier.

Benamou J. D., Brenier Y. (2000). A computational fluid mechanics solution to the Monge-Kantorovich mass transfer problem. Numerische Mathematik, 84(3), 375–393.

Geodesic interpolation: Wasserstein distance

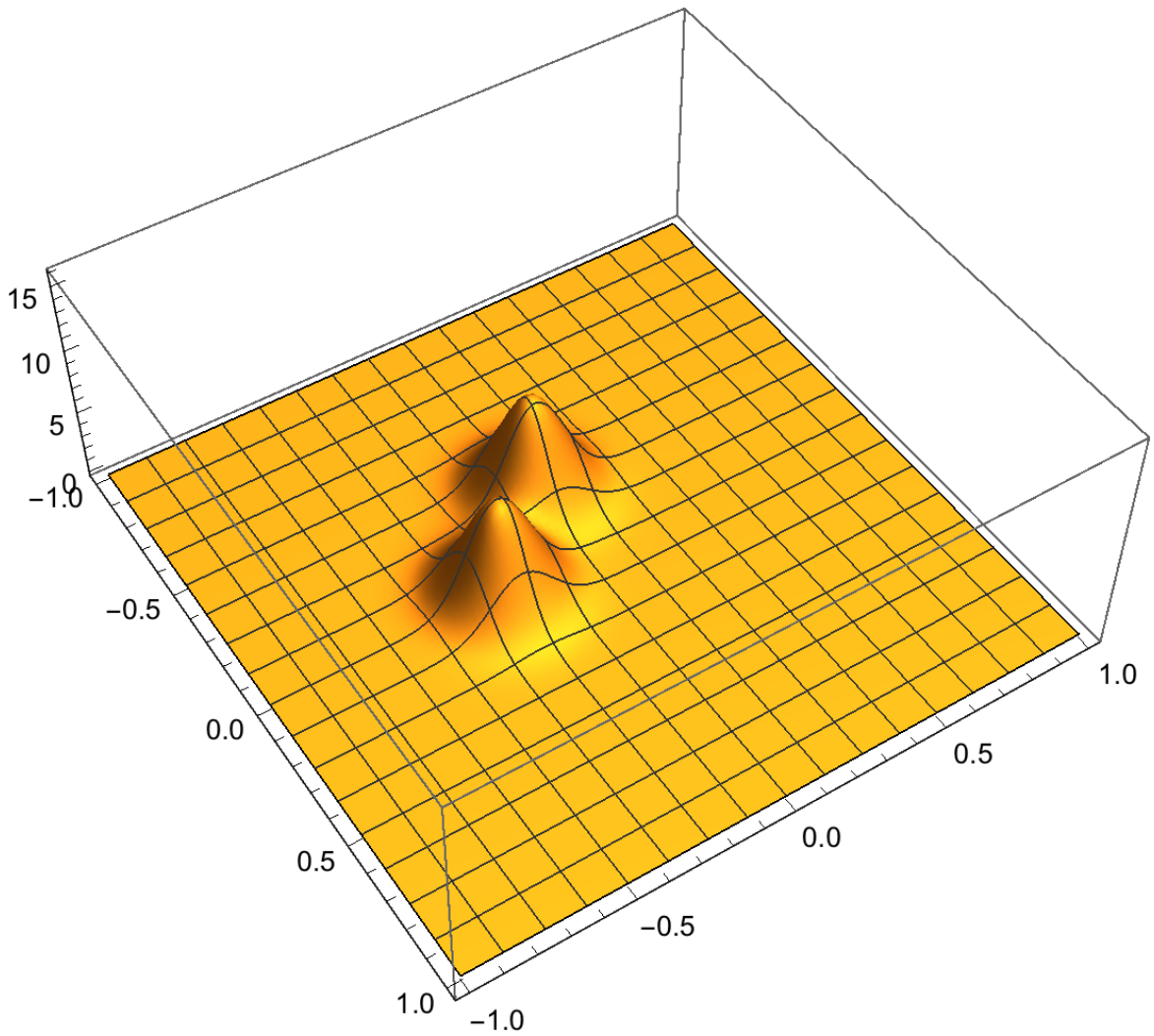

Institut de Mathématiques de Bordeaux

informatics mathematics

Geodesic interpolation: Wasserstein distance

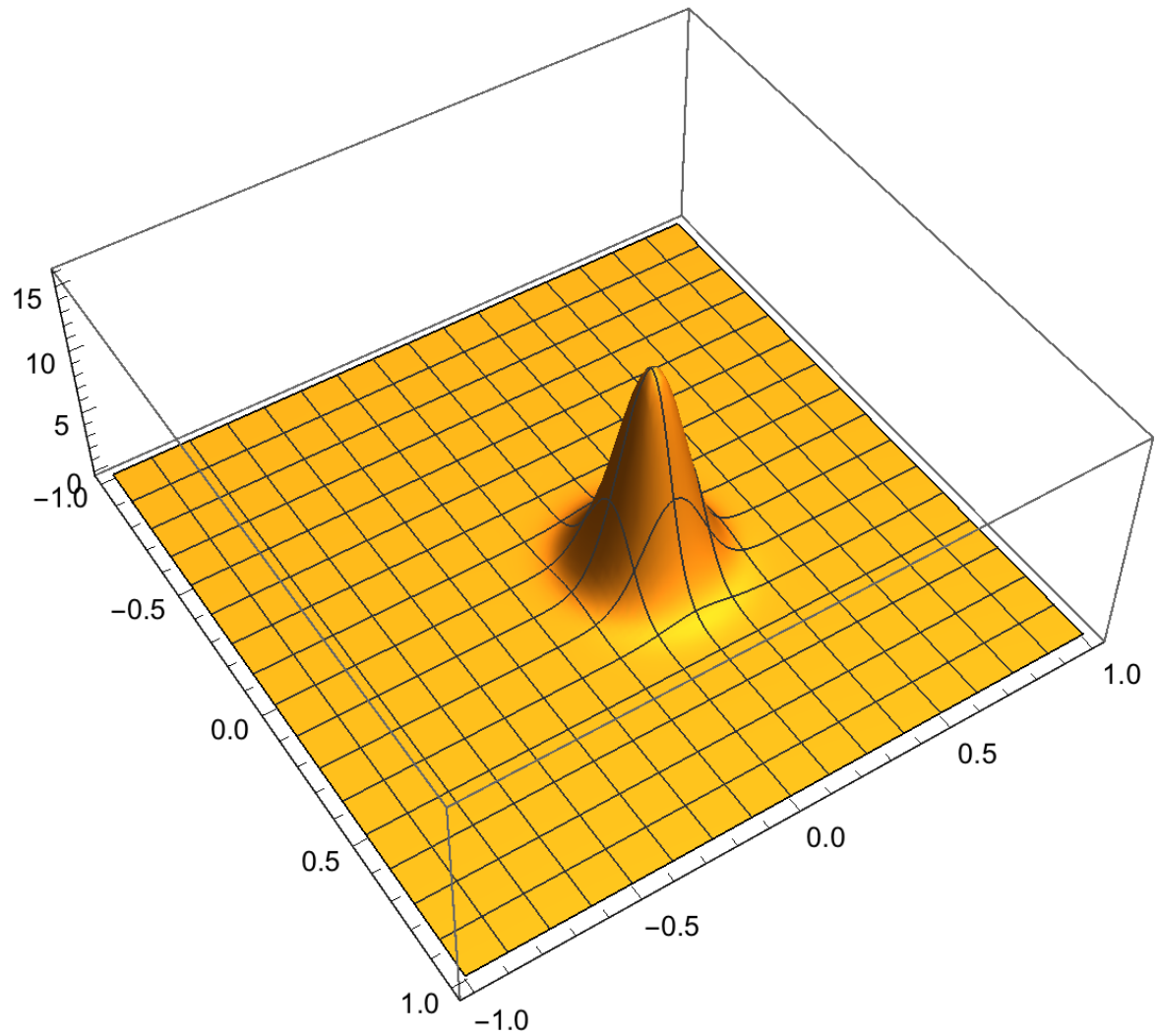

Institut de Mathématiques de Bordeaux

informatics mathematics

Geodesic interpolation: Wasserstein distance

A. Bouharguane, A. Iollo, L. Weynans. Numerical solution of the Monge-Kantorovich problem by density lift-up continuation. ESAIM: Mathematical Modelling and Numerical Analysis, 49 (6), 2015.

Institut de Mathématiques de Bordeaux

informatics mathematics

BGK equation: model reduction and OT

BGK kinetic model

Linear transport in microscopic velocity space with non-linear relaxation to equilibrium

$$\frac{\partial f}{\partial t}(\mathbf{x},\xi,t) + \xi \cdot \nabla_{\mathbf{x}} f(\mathbf{x},\xi,t) = \frac{M_f(\mathbf{x},\xi,t) - f(\mathbf{x},\xi,t)}{\tau(\mathbf{x},t)}$$

f is the density distribution function. Maxwell equilibrium distribution function:

$$M_f(\mathbf{x},\xi,t) = \frac{\rho(\mathbf{x},t)}{(2\pi T(\mathbf{x},t))^{\frac{3}{2}}} \exp\left(-\frac{|\xi - U(\mathbf{x},t)|^2}{2T(\mathbf{x},t)}\right)$$

Institut de Mathématiques de Bordeaux

informatics mathematics

BGK kinetic model

Linear transport in microscopic velocity space with non-linear relaxation to equilibrium

$$\frac{\partial f}{\partial t}(\mathbf{x},\xi,t) + \xi \cdot \nabla_{\mathbf{x}} f(\mathbf{x},\xi,t) = \frac{M_f(\mathbf{x},\xi,t) - f(\mathbf{x},\xi,t)}{\tau(\mathbf{x},t)}$$

f is the density distribution function. Maxwell equilibrium distribution function:

$$M_f(\mathbf{x},\xi,t) = \frac{\rho(\mathbf{x},t)}{(2\pi T(\mathbf{x},t))^{\frac{3}{2}}} \exp\left(-\frac{|\xi - U(\mathbf{x},t)|^2}{2T(\mathbf{x},t)}\right)$$

The macroscopic variables are:

$$\int_{\mathbb{R}^3} f(\mathbf{x},\xi,t) \begin{pmatrix} 1 \\ \xi \\ \frac{|\xi|^2}{2} \end{pmatrix} \mathrm{d}\xi = \begin{pmatrix} \rho(\mathbf{x},t) \\ \rho(\mathbf{x},t)U(\mathbf{x},t) \\ E(\mathbf{x},t) \end{pmatrix}$$

and the temperature is: $T(\mathbf{x},t) = \frac{2E(\mathbf{x},t)}{3\rho(\mathbf{x},t)} - \frac{|U(\mathbf{x},t)|^2}{3}$

Institut de Mathématiques de Bordeaux

informatics mathematics

Offline phase: Sampling of the BGK equation

High-fidelity simulations provide snapshots of the distribution functions:

$$S^{\text{hf}} = \left\{ f(\mathbf{x}_i, \xi, t_k) \right\}_{\substack{1 \le i \le N_{\mathbf{x}} \\ 1 \le k \le N_t}} \bigcup \left\{ M_f(\mathbf{x}_i, \xi, t_k) \right\}_{\substack{1 \le i \le N_{\mathbf{x}} \\ 1 \le k \le N_t}}$$

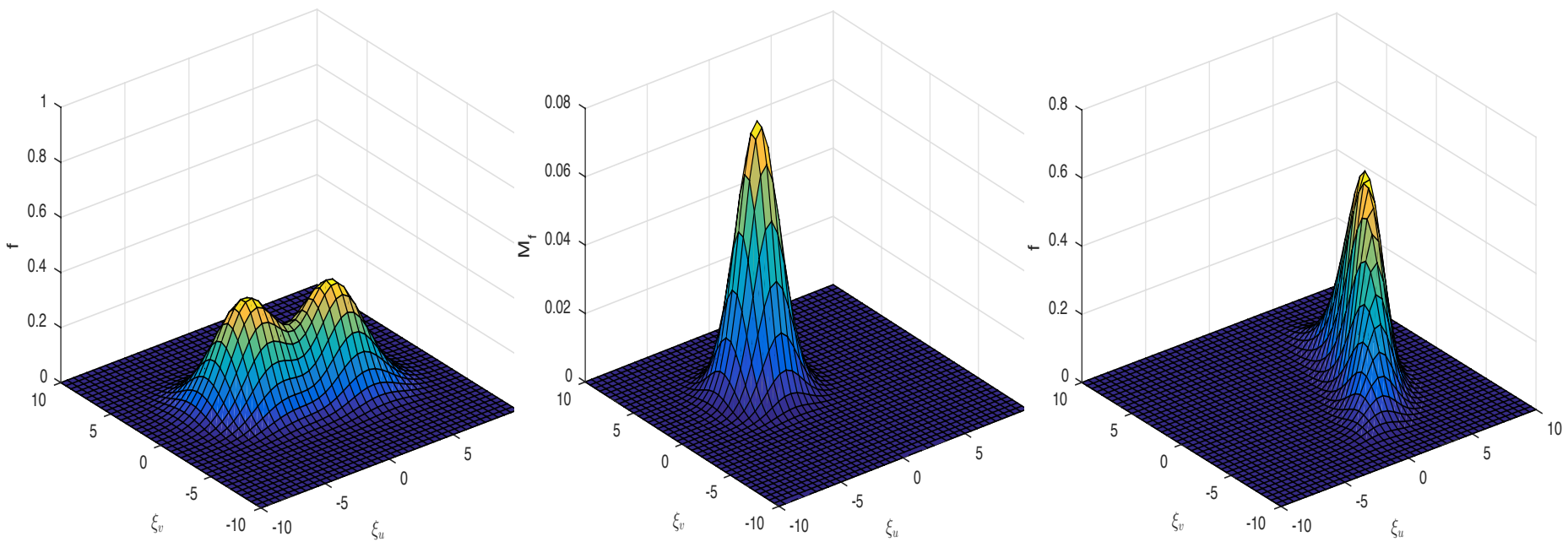

Institut de Mathématiques de Bordeaux

informatics mathematics Inria

Offline phase: Optimal Transportation

Optimal transportation provides additional low-fidelity snapshots by interpolating the snapshots of S^{hf} to complete the sampling:

$$S = S^{\text{hf}} \cup S^{\text{lf}}$$

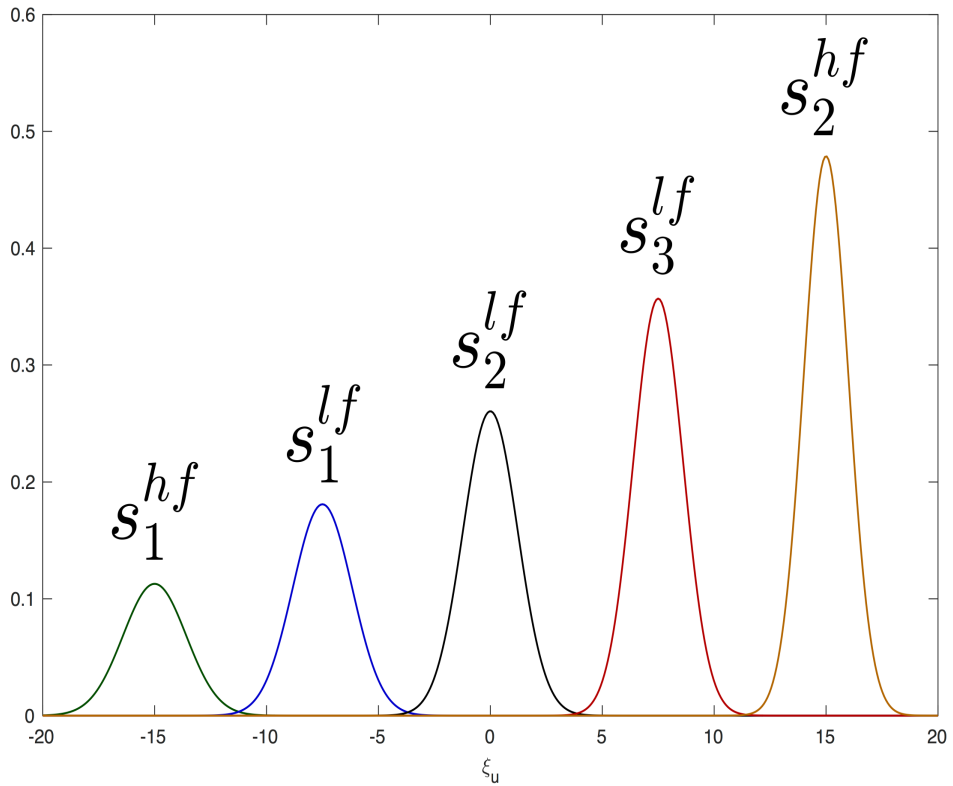

Offline phase: POD

$$\underset{\Phi_1,\dots,\Phi_{N_{pod}}}{\text{maximize}} \sum_{l=1}^{N_{snaps}} \sum_{n=1}^{N_{pod}} \left(\int_{\mathbb{R}^3} s_l(\xi)\Phi_n(\xi)\,\mathrm{d}\xi \right)^2$$

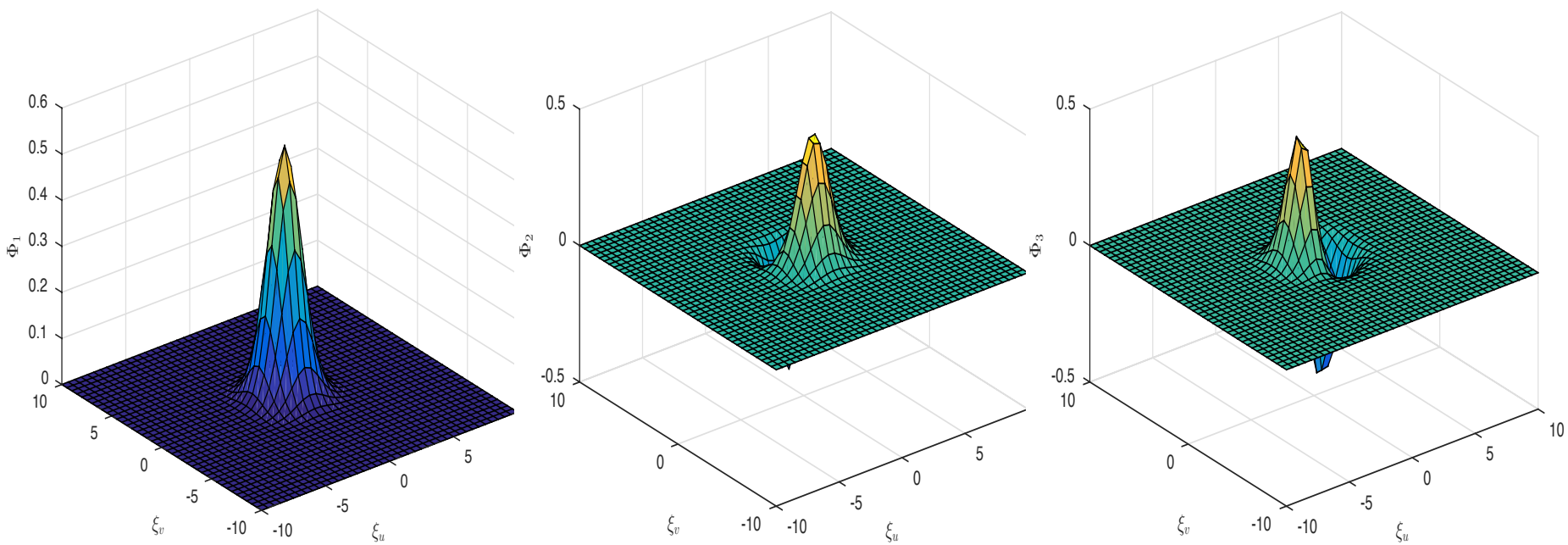

Model reduction and Galerkin orthogonality

The distribution functions are represented by a small number of basis functions $\Phi_n(\xi)$ computed offline:

$$\widetilde{f}(\mathbf{x},\xi,t) = \sum_{n=1}^{N_{pod}} a_n^f(\mathbf{x},t)\Phi_n(\xi) \qquad \widetilde{M_f}(\mathbf{x},\xi,t) = \sum_{n=1}^{N_{pod}} a_n^M(\mathbf{x},t)\Phi_n(\xi)$$

Institut de Mathématiques de Bordeaux

informatics mathematics

Model reduction and Galerkin orthogonality

The distribution functions are represented by a small number of basis functions $\Phi_n(\xi)$ computed offline:

$$\widetilde{f}(\mathbf{x},\xi,t) = \sum_{n=1}^{N_{pod}} a_n^f(\mathbf{x},t)\Phi_n(\xi) \qquad \widetilde{M_f}(\mathbf{x},\xi,t) = \sum_{n=1}^{N_{pod}} a_n^M(\mathbf{x},t)\Phi_n(\xi)$$

Residual equation

$$\mathcal{R}(\mathbf{x},\xi,t) = \frac{\partial \widetilde{f}}{\partial t}(\mathbf{x},\xi,t) + \xi \cdot \nabla_{\mathbf{x}} \widetilde{f}(\mathbf{x},\xi,t) - \frac{\widetilde{M_f}(\mathbf{x},\xi,t) - \widetilde{f}(\mathbf{x},\xi,t)}{\tau(\mathbf{x},t)}$$

Model reduction and Galerkin orthogonality

The distribution functions are represented by a small number of basis functions $\Phi_n(\xi)$ computed offline:

$$\widetilde{f}(\mathbf{x},\xi,t) = \sum_{n=1}^{N_{pod}} a_n^f(\mathbf{x},t)\Phi_n(\xi) \qquad \widetilde{M_f}(\mathbf{x},\xi,t) = \sum_{n=1}^{N_{pod}} a_n^M(\mathbf{x},t)\Phi_n(\xi)$$

Residual equation

$$\mathcal{R}(\mathbf{x},\xi,t) = \frac{\partial \widetilde{f}}{\partial t}(\mathbf{x},\xi,t) + \xi \cdot \nabla_{\mathbf{x}} \widetilde{f}(\mathbf{x},\xi,t) - \frac{\widetilde{M_f}(\mathbf{x},\xi,t) - \widetilde{f}(\mathbf{x},\xi,t)}{\tau(\mathbf{x},t)}$$

Orthogonality in the microscopic velocity space of $\mathcal{R}(\mathbf{x},\xi,t)$ to the subspace spanned by the columns of $\mathbf{\Phi}(\xi)$, $\Phi_n(\xi)$, $n = 1,\ldots,N_{pod}$:

$$< \mathcal{R}(\mathbf{x},\xi,t), \mathbf{\Phi}(\xi) >= 0$$

Institut de Mathématiques de Bordeaux

informatics mathematics

Online phase

$$
\begin{cases}
\dfrac{\partial a_1^f}{\partial t} + \displaystyle\sum_{n=1}^{N_{pod}} A_{1,n} \dfrac{\partial a_n^f}{\partial x} + \mathring{A}_{1,n} \dfrac{\partial a_n^f}{\partial y} + \overset{\star}{A}_{1,n} \dfrac{\partial a_n^f}{\partial z} = \dfrac{a_1^M - a_1^f}{\tau} \\
\dfrac{\partial a_2^f}{\partial t} + \displaystyle\sum_{n=1}^{N_{pod}} A_{2,n} \dfrac{\partial a_n^f}{\partial x} + \mathring{A}_{2,n} \dfrac{\partial a_n^f}{\partial y} + \overset{\star}{A}_{2,n} \dfrac{\partial a_n^f}{\partial z} = \dfrac{a_2^M - a_2^f}{\tau} \\
\vdots \\
\dfrac{\partial a_{N_{pod}}^f}{\partial t} + \displaystyle\sum_{n=1}^{N_{pod}} A_{N_{pod},n} \dfrac{\partial a_n^f}{\partial x} + \mathring{A}_{N_{pod},n} \dfrac{\partial a_n^f}{\partial y} + \overset{\star}{A}_{N_{pod},n} \dfrac{\partial a_n^f}{\partial z} = \dfrac{a_{N_{pod}}^M - a_{N_{pod}}^f}{\tau}
\end{cases}
$$

where $A_{n,m} = \int_{\mathbb{R}^3} \xi_u \Phi_n(\xi)\Phi_m(\xi)\,\mathrm{d}\xi$, $\mathring{A}_{n,m} = \int_{\mathbb{R}^3} \xi_v \Phi_n(\xi)\Phi_m(\xi)\,\mathrm{d}\xi$ and $\overset{\star}{A}_{n,m} = \int_{\mathbb{R}^3} \xi_w \Phi_n(\xi)\Phi_m(\xi)\,\mathrm{d}\xi$.

Institut de Mathématiques de Bordeaux

informatics mathematics

Online phase

$$
\begin{cases}
\dfrac{\partial a_1^f}{\partial t} + \displaystyle\sum_{n=1}^{N_{pod}} A_{1,n} \dfrac{\partial a_n^f}{\partial x} + \mathring{A}_{1,n} \dfrac{\partial a_n^f}{\partial y} + \overset{\star}{A}_{1,n} \dfrac{\partial a_n^f}{\partial z} = \dfrac{a_1^M - a_1^f}{\tau} \\
\dfrac{\partial a_2^f}{\partial t} + \displaystyle\sum_{n=1}^{N_{pod}} A_{2,n} \dfrac{\partial a_n^f}{\partial x} + \mathring{A}_{2,n} \dfrac{\partial a_n^f}{\partial y} + \overset{\star}{A}_{2,n} \dfrac{\partial a_n^f}{\partial z} = \dfrac{a_2^M - a_2^f}{\tau} \\
\vdots \\
\dfrac{\partial a_{N_{pod}}^f}{\partial t} + \displaystyle\sum_{n=1}^{N_{pod}} A_{N_{pod},n} \dfrac{\partial a_n^f}{\partial x} + \mathring{A}_{N_{pod},n} \dfrac{\partial a_n^f}{\partial y} + \overset{\star}{A}_{N_{pod},n} \dfrac{\partial a_n^f}{\partial z} = \dfrac{a_{N_{pod}}^M - a_{N_{pod}}^f}{\tau}
\end{cases}
$$

where $A_{n,m} = \int_{\mathbb{R}^3} \xi_u \Phi_n(\xi)\Phi_m(\xi)\,\mathrm{d}\xi$, $\mathring{A}_{n,m} = \int_{\mathbb{R}^3} \xi_v \Phi_n(\xi)\Phi_m(\xi)\,\mathrm{d}\xi$ and $\overset{\star}{A}_{n,m} = \int_{\mathbb{R}^3} \xi_w \Phi_n(\xi)\Phi_m(\xi)\,\mathrm{d}\xi$.

A, $\mathring{A}$ and $\overset{\star}{A}$ are real and symmetric $\Rightarrow$ **the system is hyperbolic.**

Institut de Mathématiques de Bordeaux

informatics mathematics

Online phase

Non-conservation of the moments:

$$\int_{\mathbb{R}^3} \widetilde{M_f}(\mathbf{x},\xi,t) \begin{pmatrix} 1 \\ \xi \\ \frac{\|\xi\|^2}{2} \end{pmatrix} \mathrm{d}\xi \neq \begin{pmatrix} \rho(\mathbf{x},t) \\ \rho(\mathbf{x},t)U(\mathbf{x},t) \\ E(\mathbf{x},t) \end{pmatrix}$$

Conservative projection:

$$\begin{cases} \underset{a_1^M,\ldots,a_{N_{pod}}^M}{\text{minimize}} & \displaystyle\int_{\mathbb{R}^3} \left(\widetilde{M_f}(\mathbf{x},\xi,t) - M_f(\mathbf{x},\xi,t)\right)^2 \mathrm{d}\xi \\ \text{subject to} & \displaystyle\int_{\mathbb{R}^3} \widetilde{M_f}(\mathbf{x},\xi,t) \begin{pmatrix} 1 \\ \xi \\ \frac{\|\xi\|^2}{2} \end{pmatrix} \mathrm{d}\xi = \begin{pmatrix} \rho(\mathbf{x},t) \\ \rho(\mathbf{x},t)U(\mathbf{x},t) \\ E(\mathbf{x},t) \end{pmatrix} \end{cases}$$

$\Rightarrow$ Linear system with explicit solution.

Institut de Mathématiques de Bordeaux

informatics mathematics Inria

Euler limit: shock wave reduced model

Shock tube solution

Sod test case with parametric initial conditions: $u_0 \in [-2, 2]$

$$\begin{cases} \rho(x,0) = 1,\ u(x,0) = u_0,\ T(x,0) = 0.5 & \text{if } x \in]0, 0.5[\\ \rho(x,0) = 0.125,\ u(x,0) = u_0,\ T(x,0) = 0.4 & \text{if } x \in [0.5, 1[\end{cases}$$

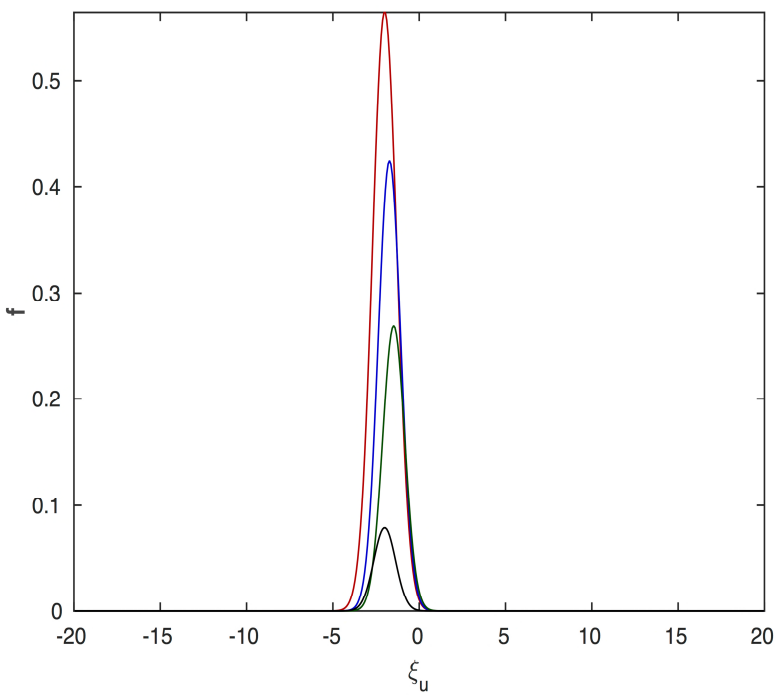

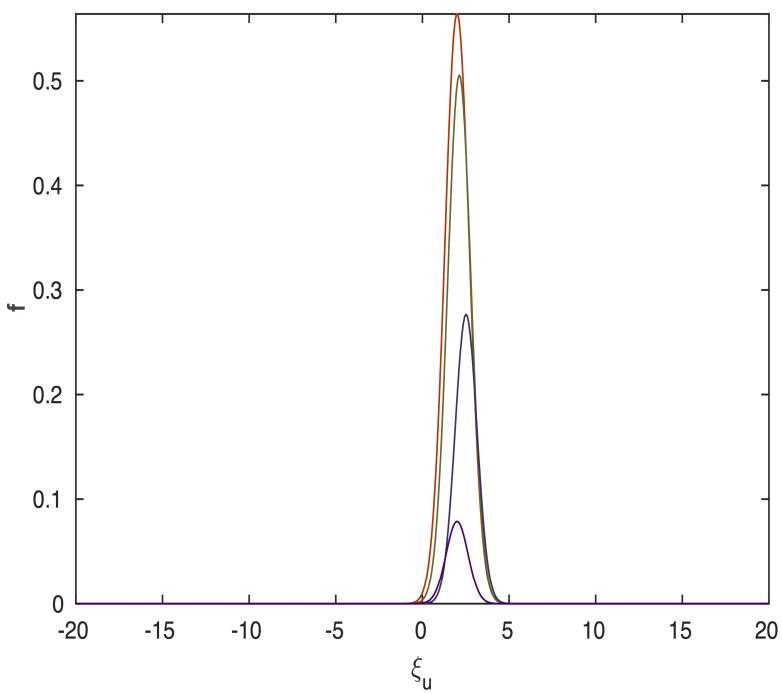

Snapshots of simulations $u_0 = -2$ (left) and $u_0 = 2$ (right).

Institut de Mathématiques de Bordeaux

informatics mathematics Inria

Shock wave prediction error

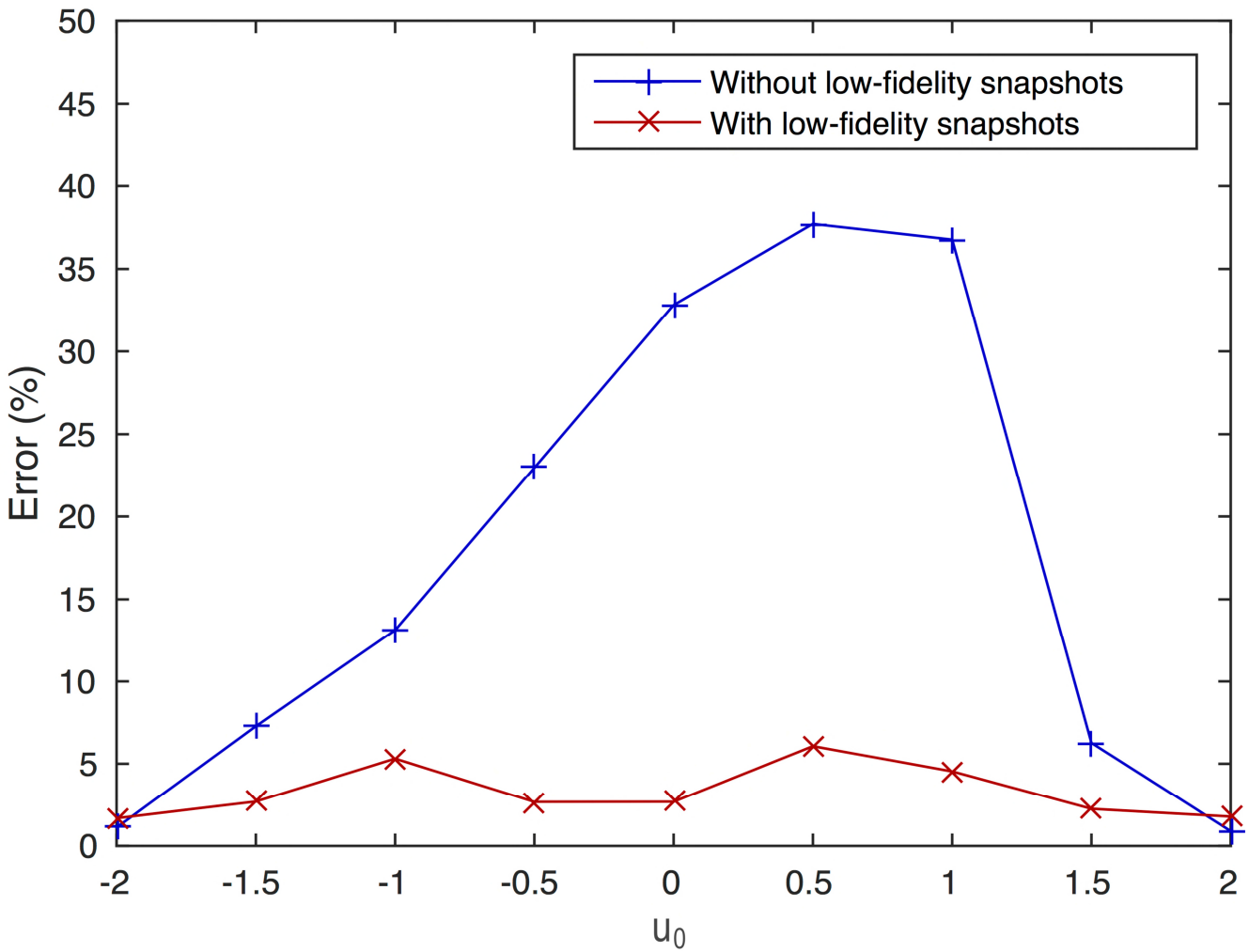

Relative error of the solution with $N_{pod} = 9$. Online computing time is divided by 20.

Rarefied flow past a flat plate

Prediction of a vortex flow as a function of the Mach number ($M_{bc} = 0.53$, $N_{pod} = 20$ and $Kn = 10^{-2}$).

Rarefied flow past a flat plate: prediction error

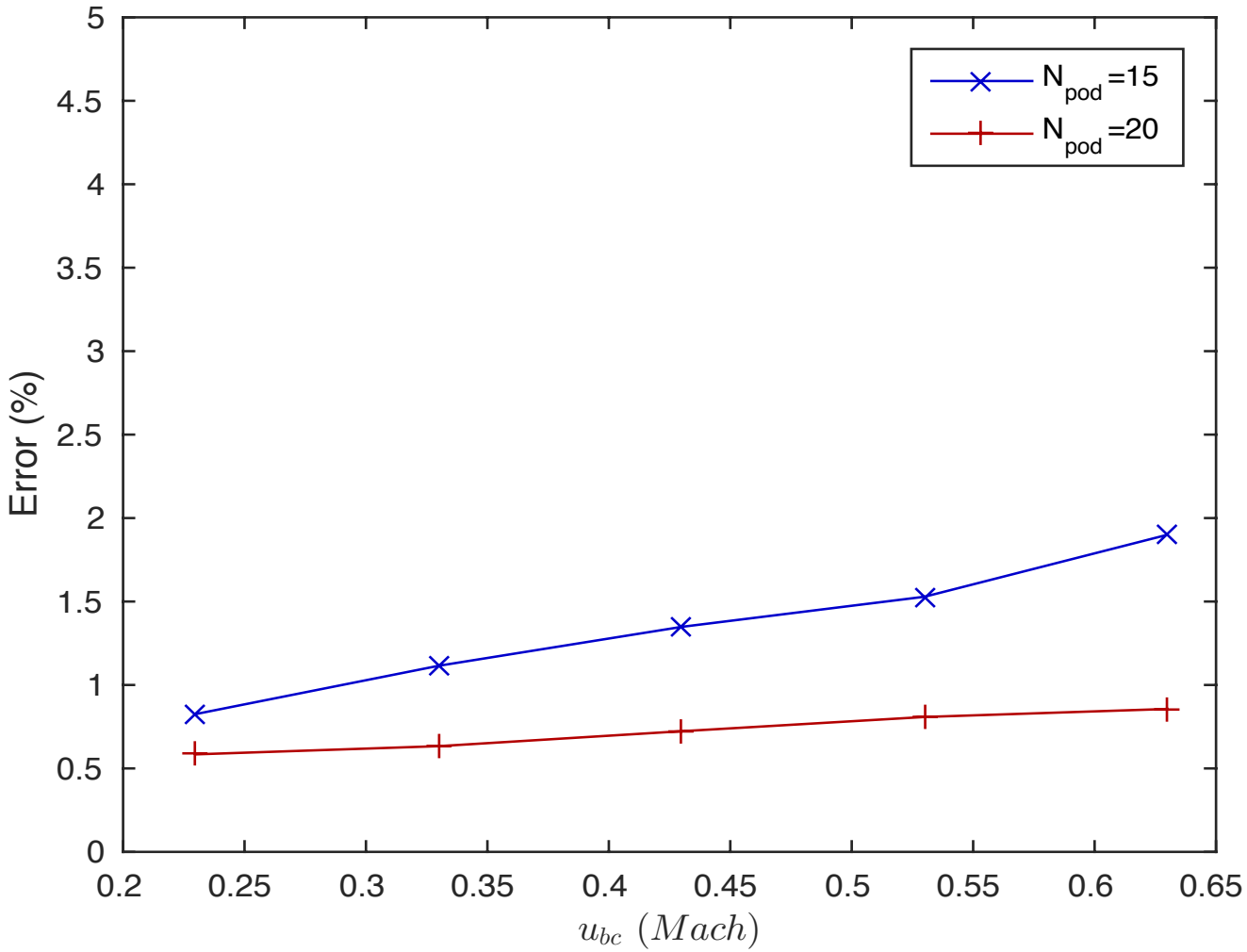

Online computing time is divided by 50 for $N_{pod} = 15$ (and by 45 for $N_{pod} = 20$) on average.

Institut de Mathématiques de Bordeaux

informatics mathematics Inria

Incompressible Navier-Stokes equations: FOM/ROM coupling

Domain decomposition

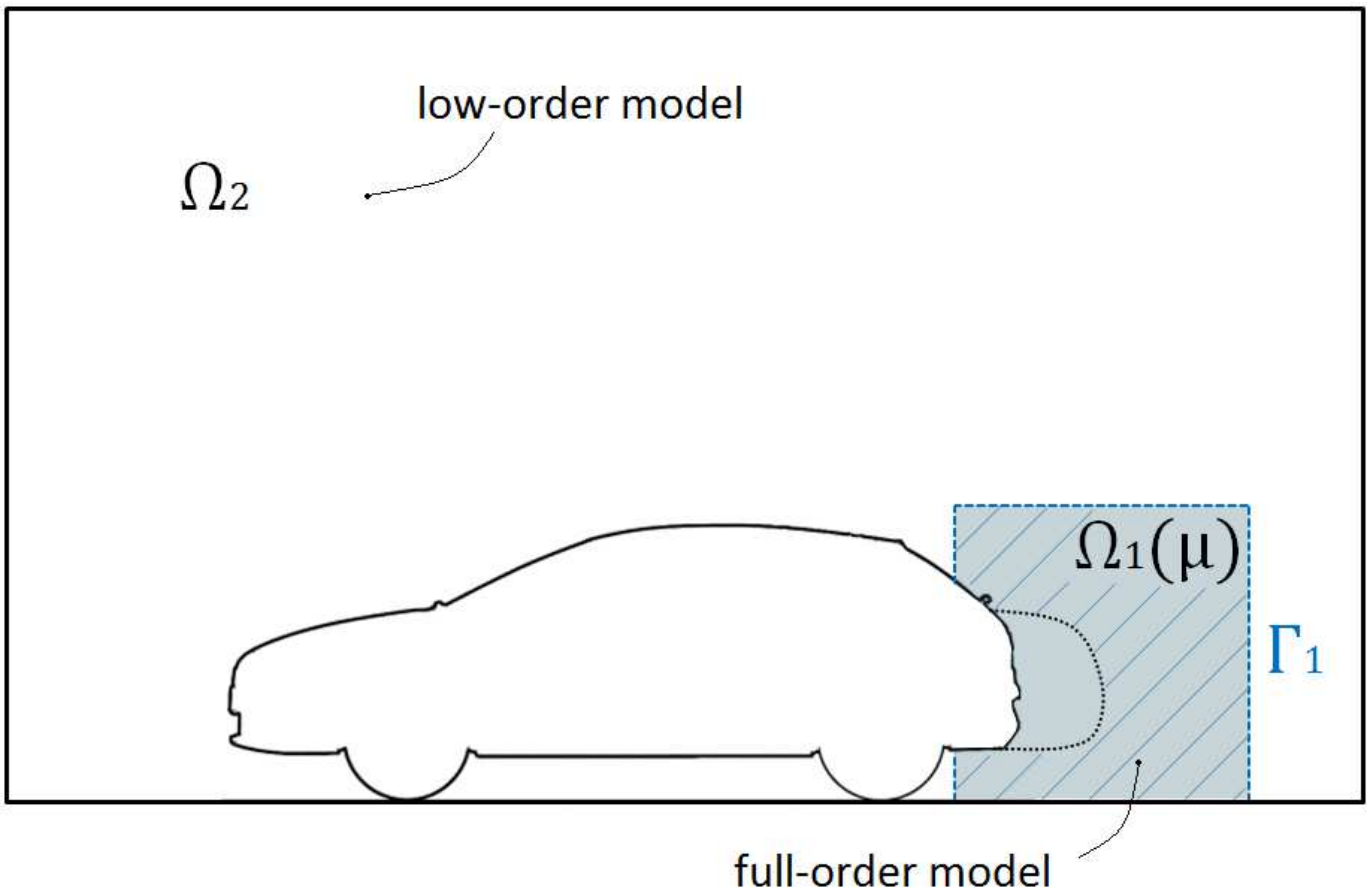

$\Omega_1(\boldsymbol{\mu})$ FOM model

Ω_2 Reduced model used to define boundary conditions on Γ_1

Domain decomposition

Stage $(\boldsymbol{u}_2, p_2) \rightarrow (\boldsymbol{u}_1, p_1)$. Given the initial condition, $(\boldsymbol{u}_2, p_2)$ in Ω_2, consider its restriction to Γ_1.
We define $(\boldsymbol{u}_1, p_1)$ as the solution of:

$$
\begin{aligned}
A(\boldsymbol{u}_1, p_1) &= 0 \qquad \text{in } \Omega_1(\boldsymbol{\mu}),\\
B(\boldsymbol{u}_1, p_1) &= 0 \qquad \text{on } \partial\Omega_1(\boldsymbol{\mu}) \cap \partial\Omega(\boldsymbol{\mu}),\\
C(\boldsymbol{u}_1, p_1) &= C(\boldsymbol{u}_2, p_2) \qquad \text{on } \Gamma_1.
\end{aligned}
$$

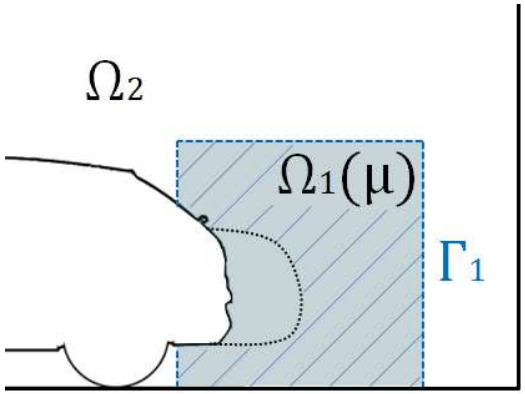

On Γ_1 we have a matching condition and $C(\boldsymbol{u}, p) = g$ denotes an admissible boundary condition for the NS.

Coupling

Stage $(\boldsymbol{u}_1, p_1) \rightarrow (\boldsymbol{u}_2, p_2)$.
Given $(\boldsymbol{u}_1, p_1)$ in $\Omega_1(\boldsymbol{\mu})$, we recover $(\boldsymbol{u}_2, p_2)_{|\Omega_{ov}}$ by projection:

$$\min_{\alpha} \| \boldsymbol{u}_1 - \sum_{i=1}^{M_r^{\varphi}} \alpha_i \boldsymbol{\varphi}_{i|\Omega_{ov}} \|^2_{\Omega_{ov}} \quad \text{and} \quad \min_{\beta} \| p_1 - \sum_{i=1}^{M_r^{\psi}} \beta_i \psi_{i|\Omega_{ov}} \|^2_{\Omega_{ov}}$$

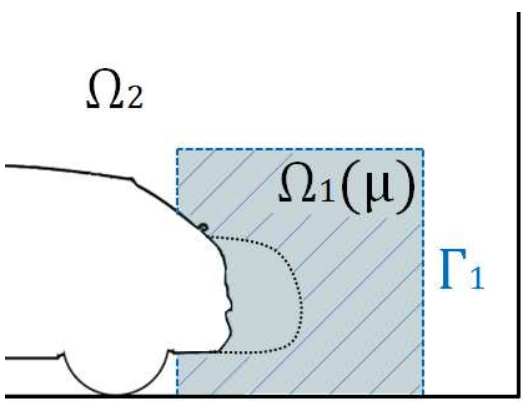

$(\boldsymbol{u}_2, p_2)_{|\Omega_{ov}}$ can be easily extended to Ω_2, but $(\boldsymbol{u}_2, p_2)$ is only required on Γ_1 during the algorithm iterations.

Convergence between data and simulation

2D DrivAer car model

Domain L×H=50m×12m, $U_\infty = 16$m/s, $l_{ref} = 4.61$m

RANS simulations: Spalart-Allmaras turbulence model at $Re = 4.87\,10^6$

FFD parametrization of car front bumper $\boldsymbol{\mu} = (\mu_0, \mu_1)$

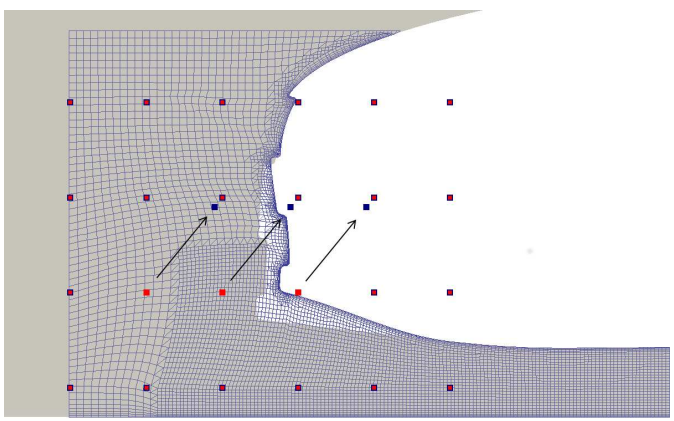

Sampling

Data driven selection of Ω_1 and Ω_2

Convergence

Institut de Mathématiques de Bordeaux

informatics mathematics Inria

Sampling

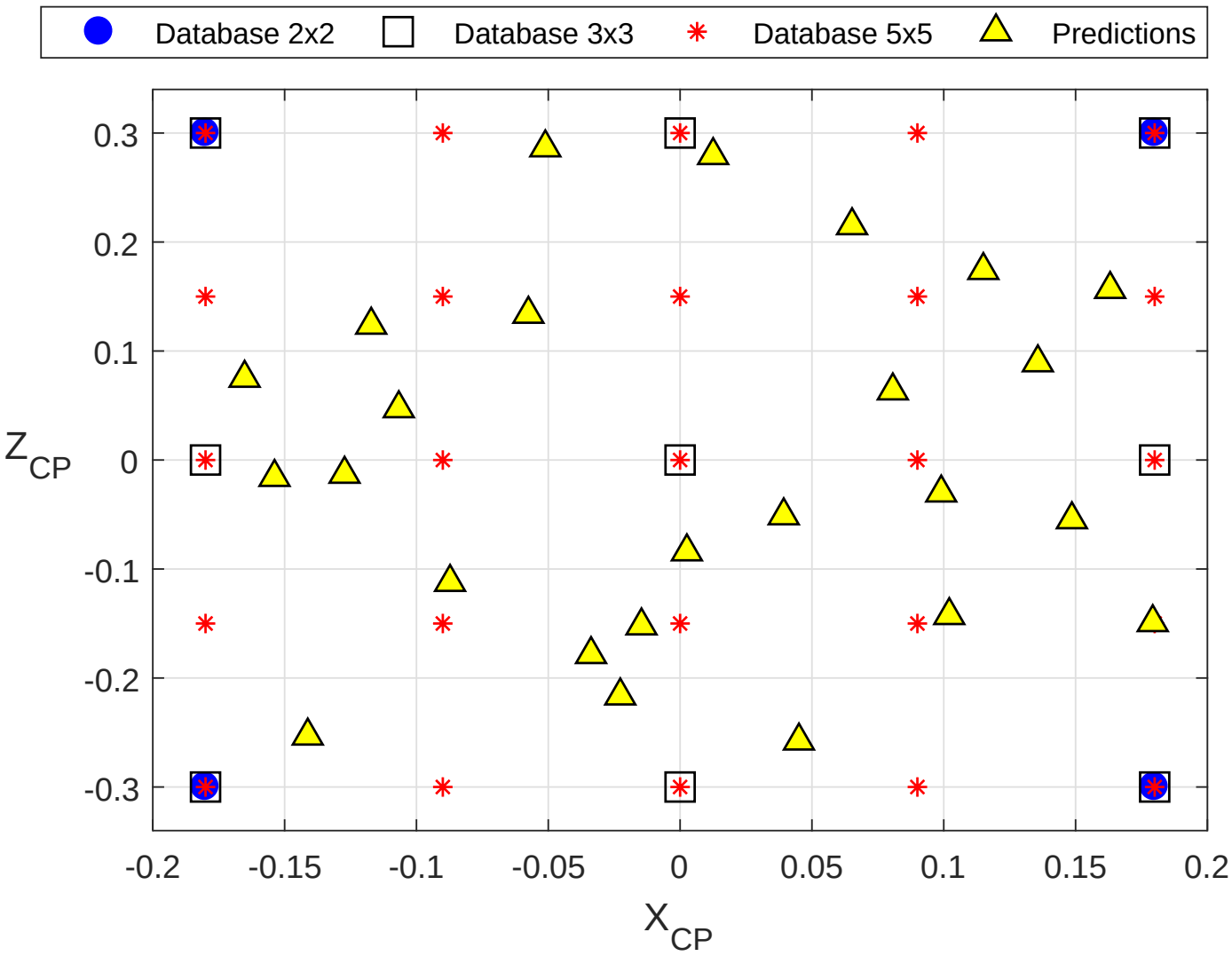
Database 2x2
Database 3x3
Database 5x5
Predictions
0.3
0.2
0.1
0
-0.1
-0.2
-0.3
Z_{CP}
-0.2
-0.15
-0.1
-0.05
0
0.05
0.1
0.15
0.2
X_{CP}

Error indicator

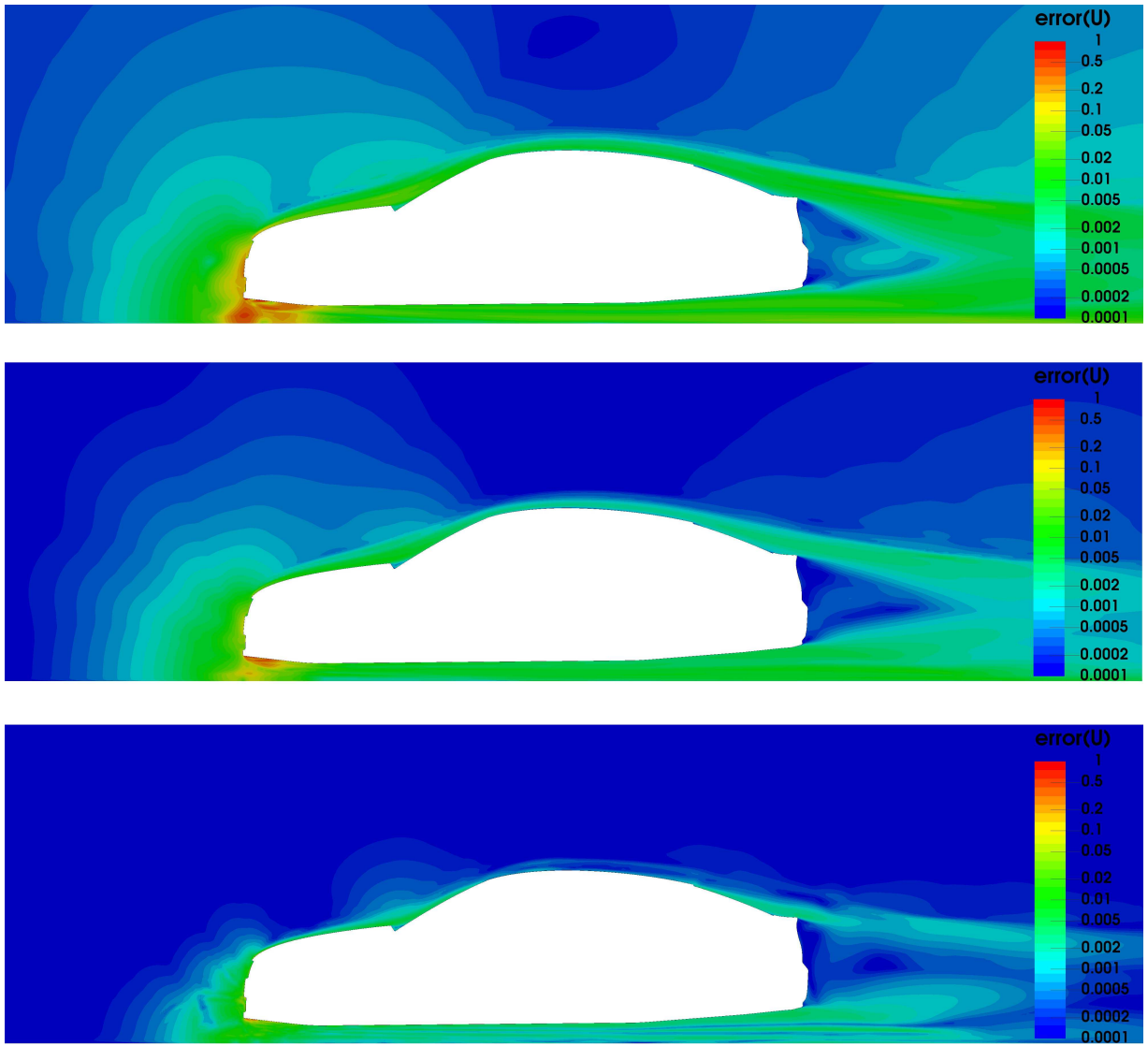

$e(\boldsymbol{x})$ on velocity for $2 \times 2, 3 \times 3, 5 \times 5$ databases

Institut de Mathématiques de Bordeaux

informatics mathematics

Decomposition threshold

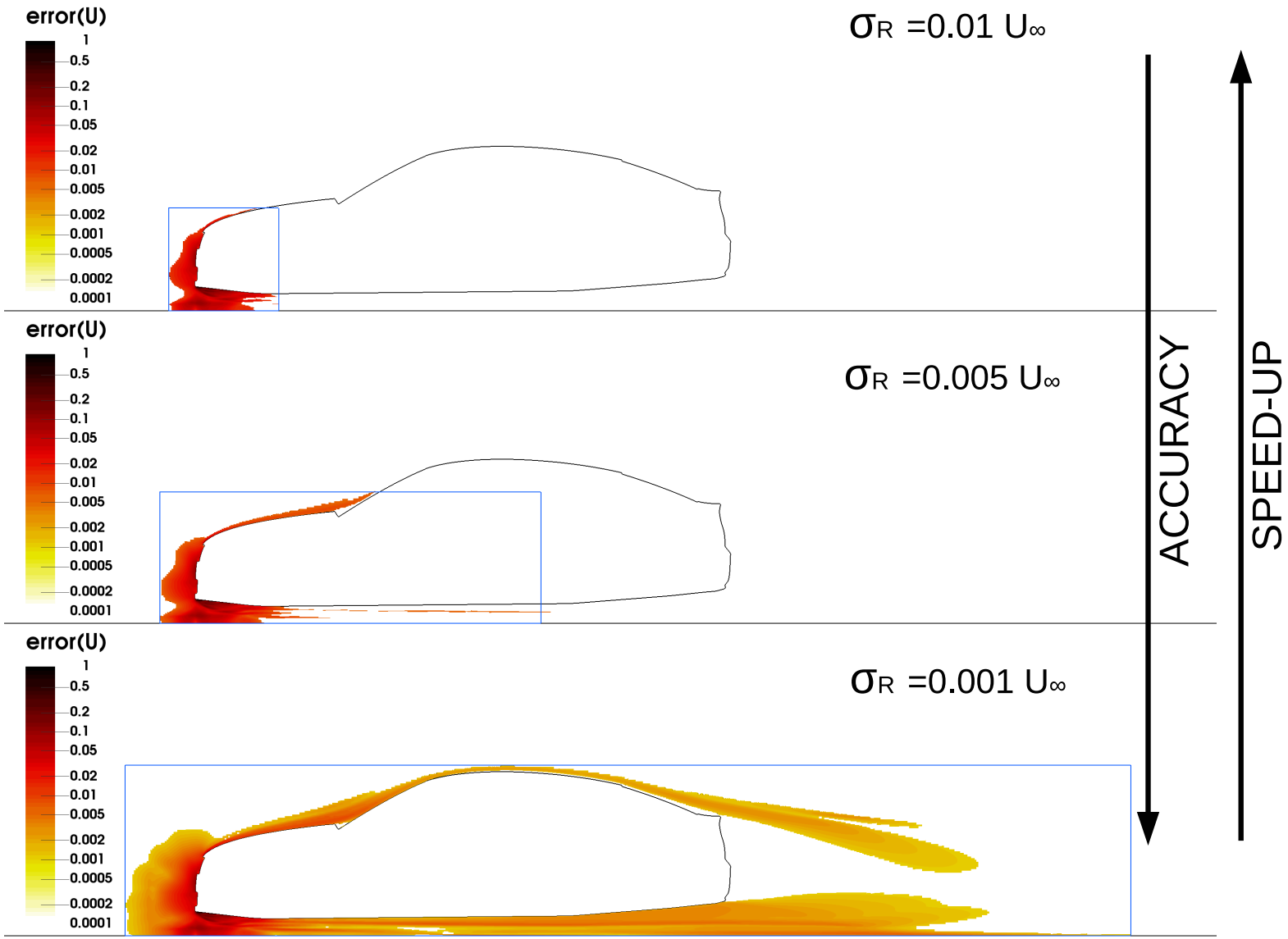

Drag coefficient

The goal function, i.e. the overall drag coefficient, is given by the sum of 2 contributions

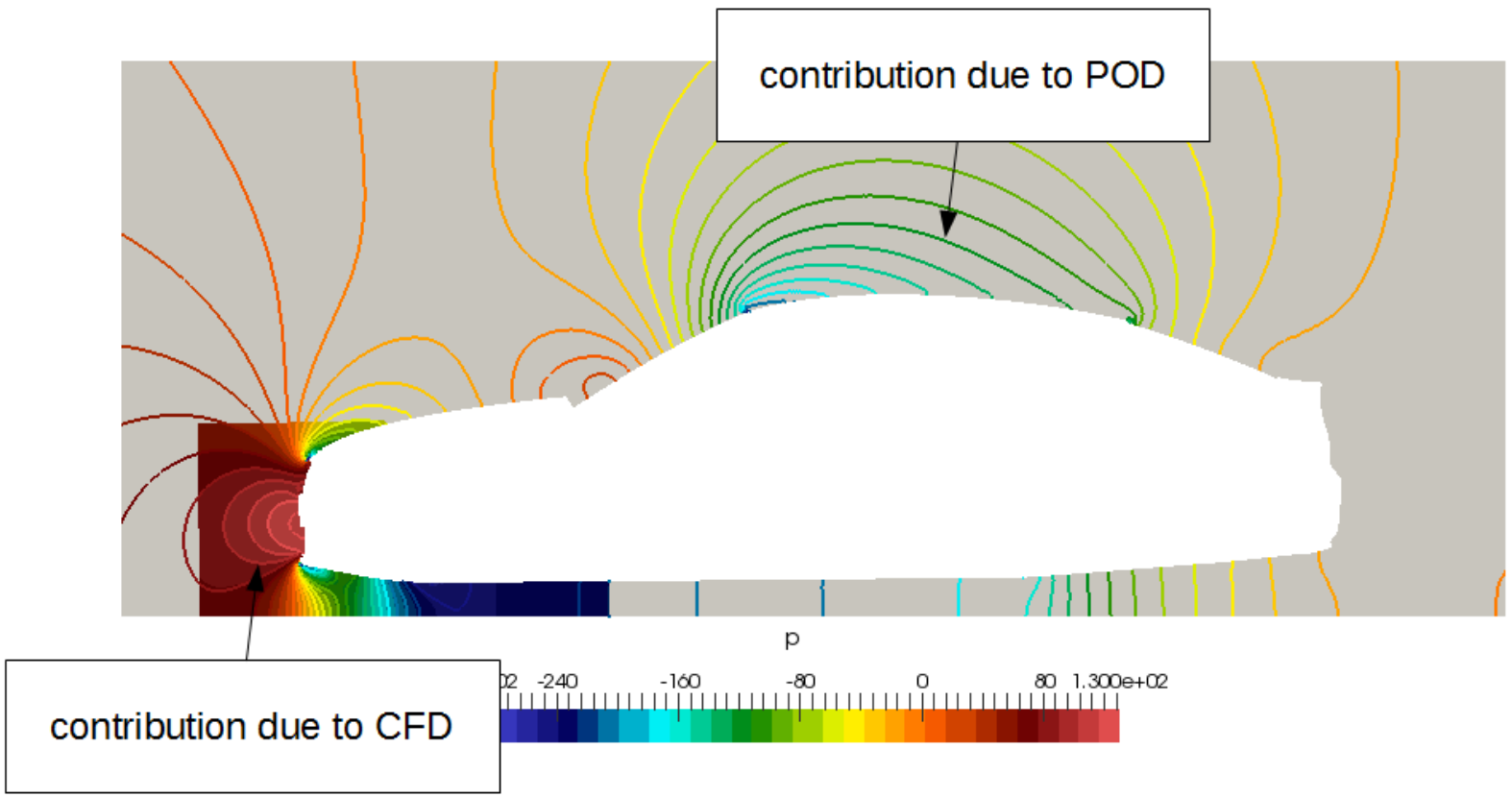

Prediction error maps

Drag coefficient error as a function of the decomposition

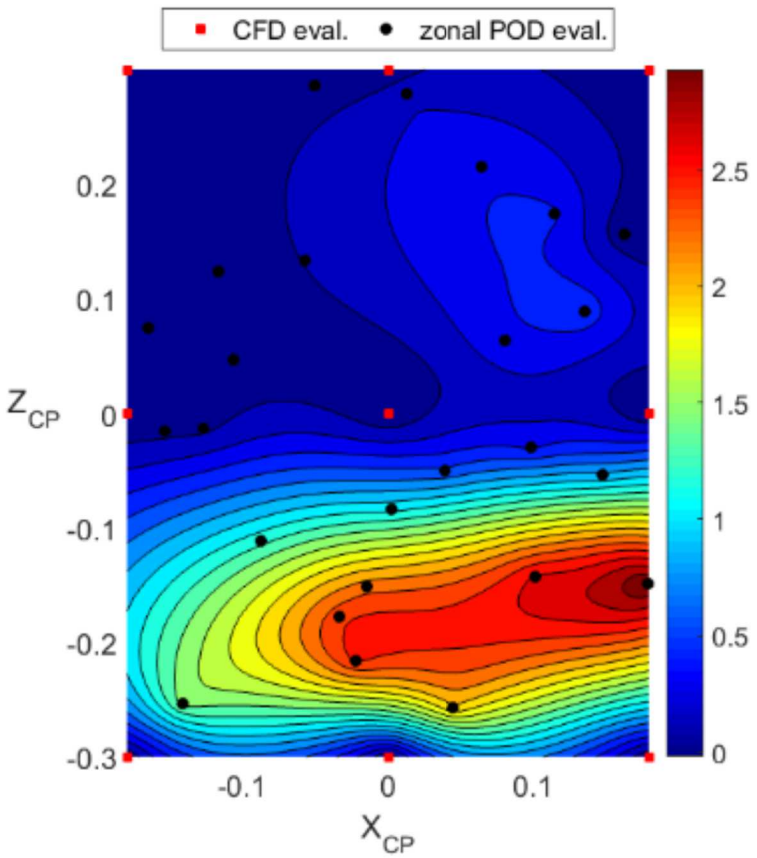

σ_R=0.01 U∞
ε=0.9341%
→ 10x speed-up factor

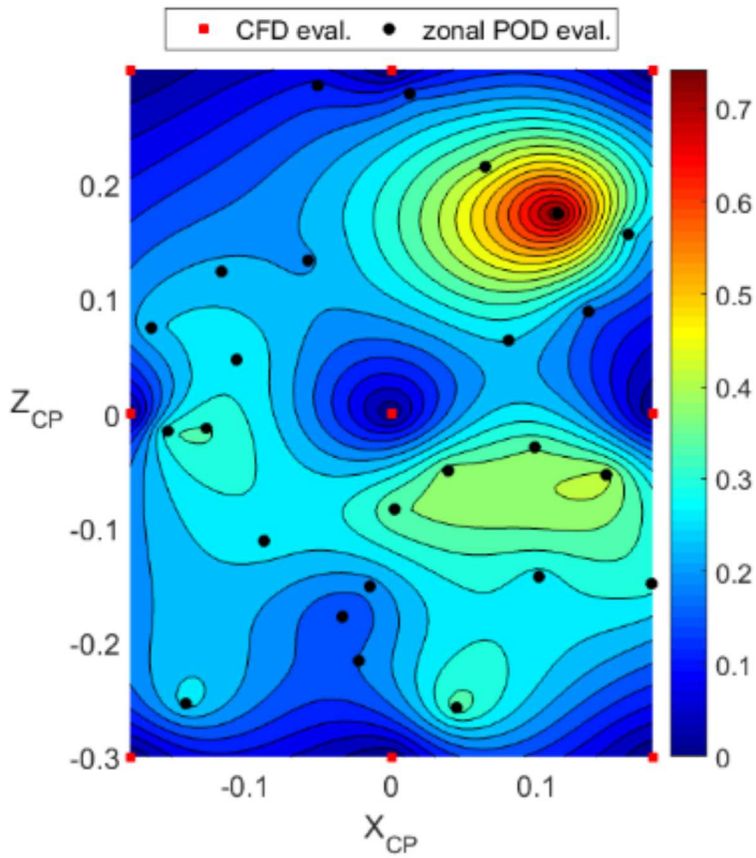

σ_R=0.001 U∞
ε=0.2992%
→ 2x speed-up factor

Institut de Mathématiques de Bordeaux

informatics mathematics Inria

Sampling

Greedy sampling vs uniform sampling

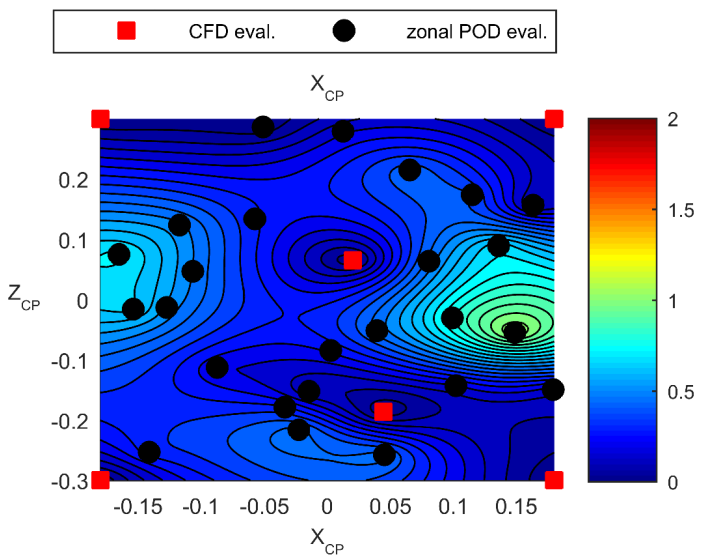

N=5
Ns=6

ε=0.4271%

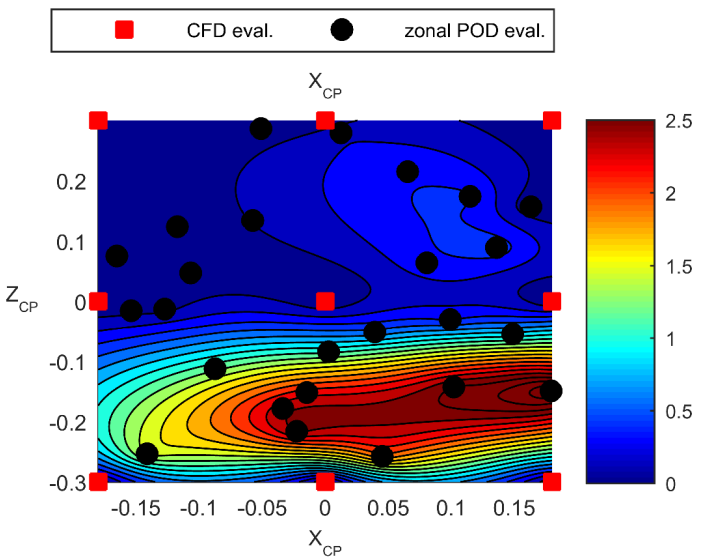

N=8
Ns=9

ε=0.9341%

the ensemble-averaged error ϵ is halved using 6 snapshots instead of 9

Institut de Mathématiques de Bordeaux

informatics mathematics

3D DrivAer model

Institut de Mathématiques de Bordeaux

informatics mathematics Inria

3D DrivAer model

Domain L×H×W=50m×12m×10m
$U_\infty = 16$m/s, $l_{ref} = 4.61$m
RANS simulations: Spalart-Allmaras turbulence model at $Re = 4.87\,10^6$
SIMPLE iterations, $1.5\,10^7$ cells

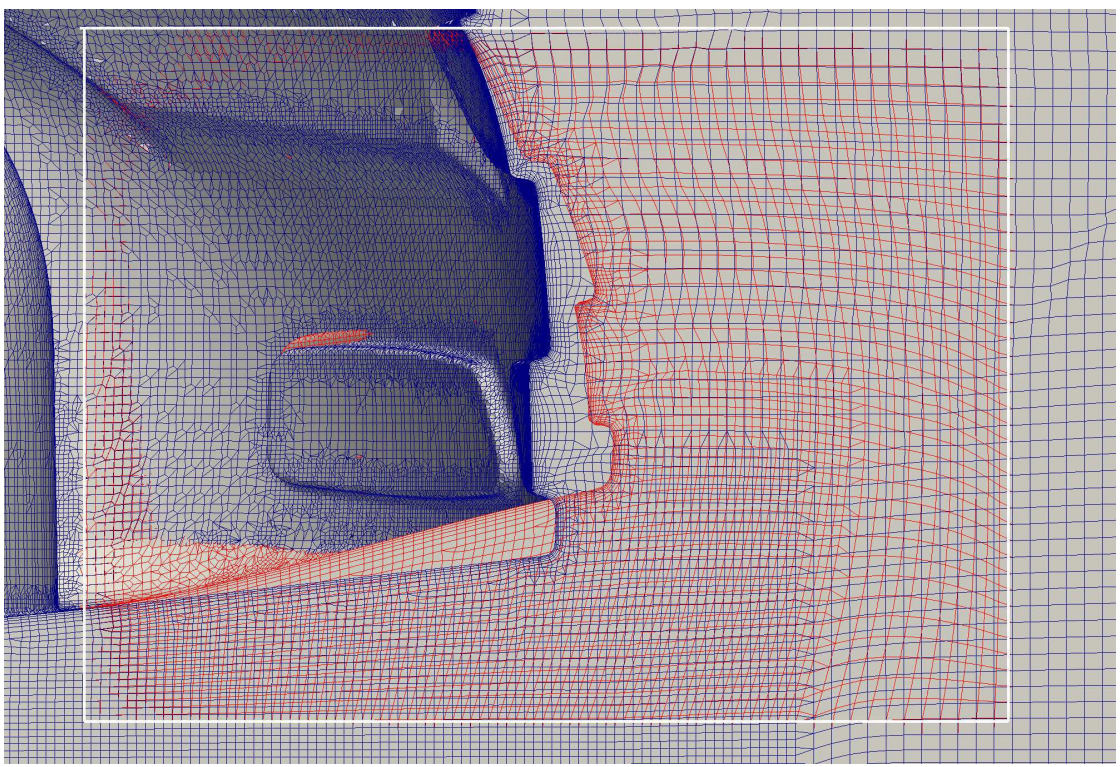

FFD parametrization of car front bumper $\boldsymbol{\mu} = (\mu_0, \mu_1)$

Institut de Mathématiques de Bordeaux

informatics mathematics Inria

Domain decomposition: error analysis

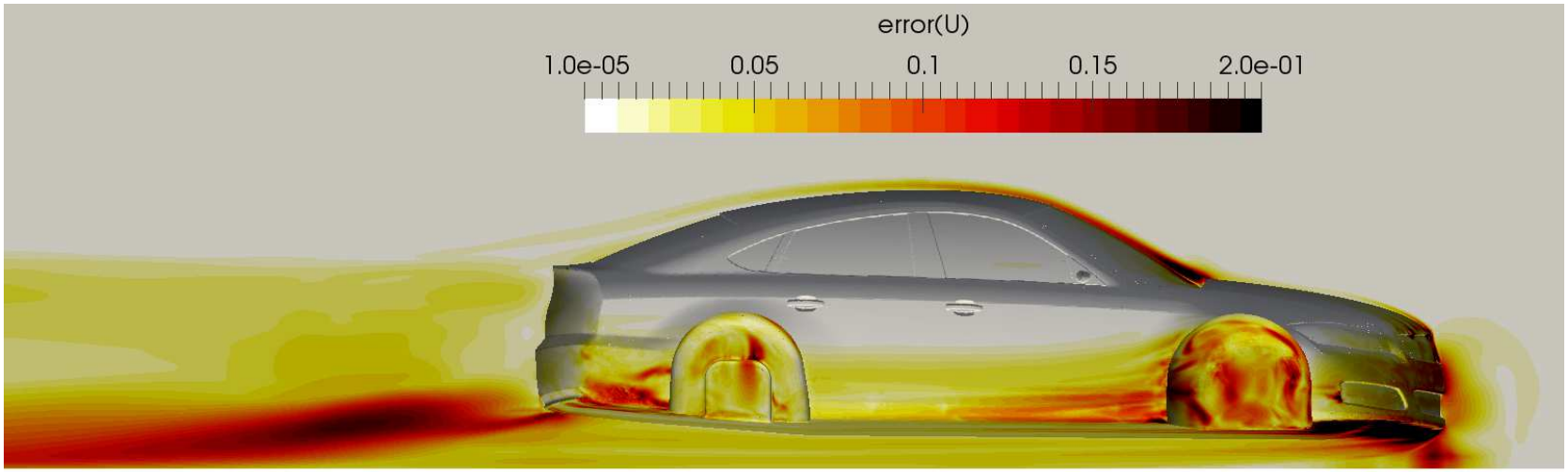

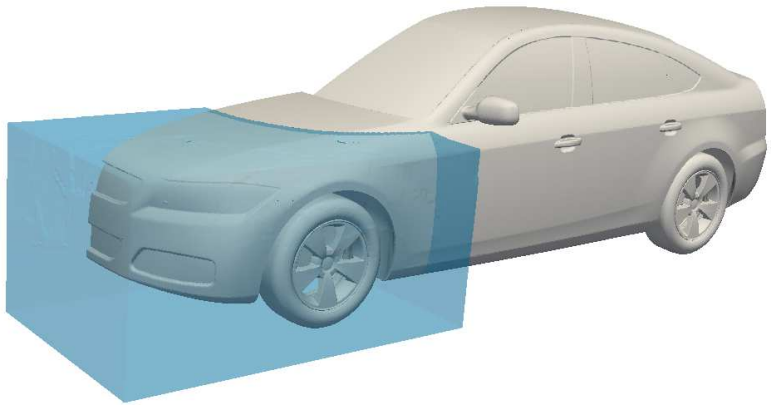

	cells	cpuh
FOM	$15 \cdot 10^6$	160
H. FOM/ROM	$2 \cdot 10^6$	20

$\sigma_R = 0.25 U_\infty \rightarrow 8\times$ speed-up factor

Institut de Mathématiques de Bordeaux

informatics mathematics

Sampling of the parameter space

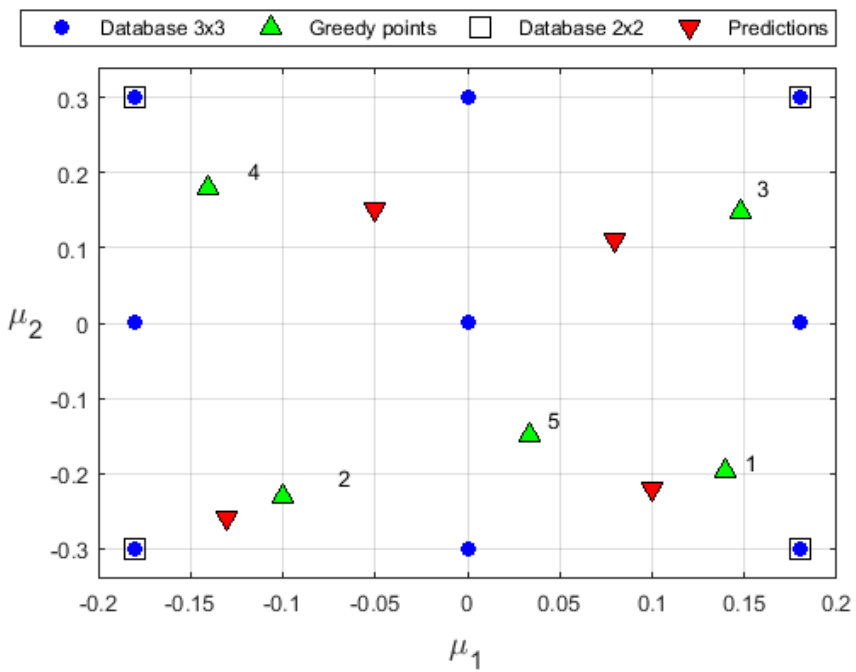

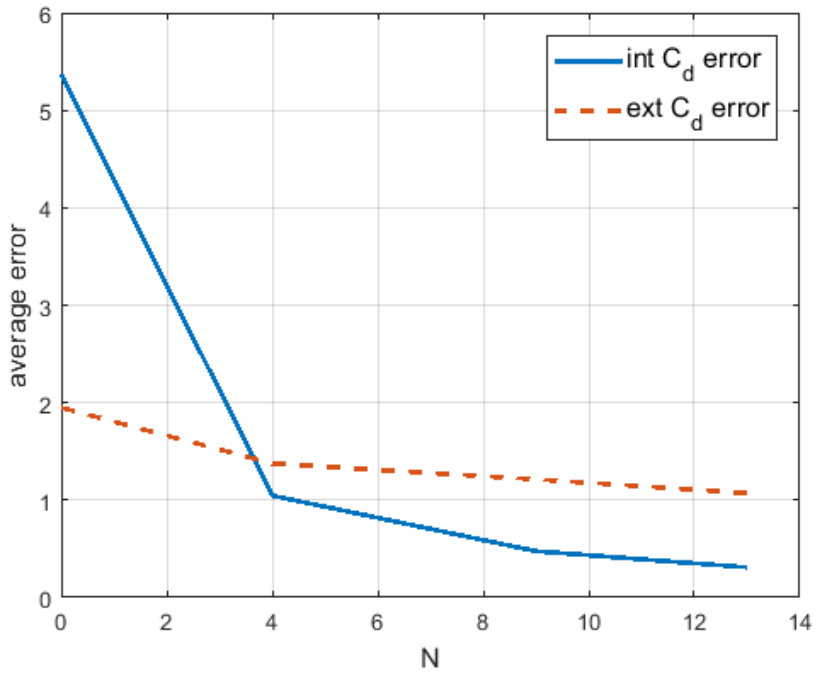

Worst prediction

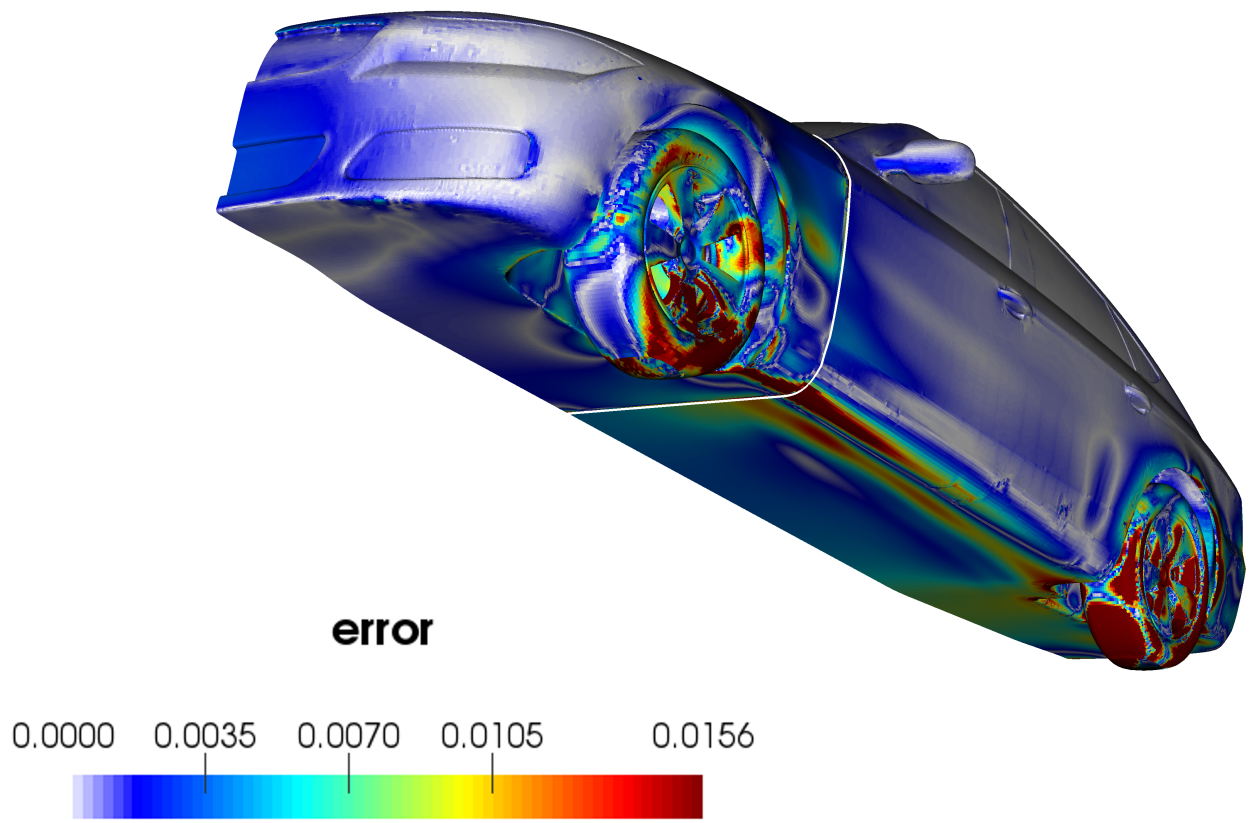

Error relative to dynamic pressure

Rear mirror design

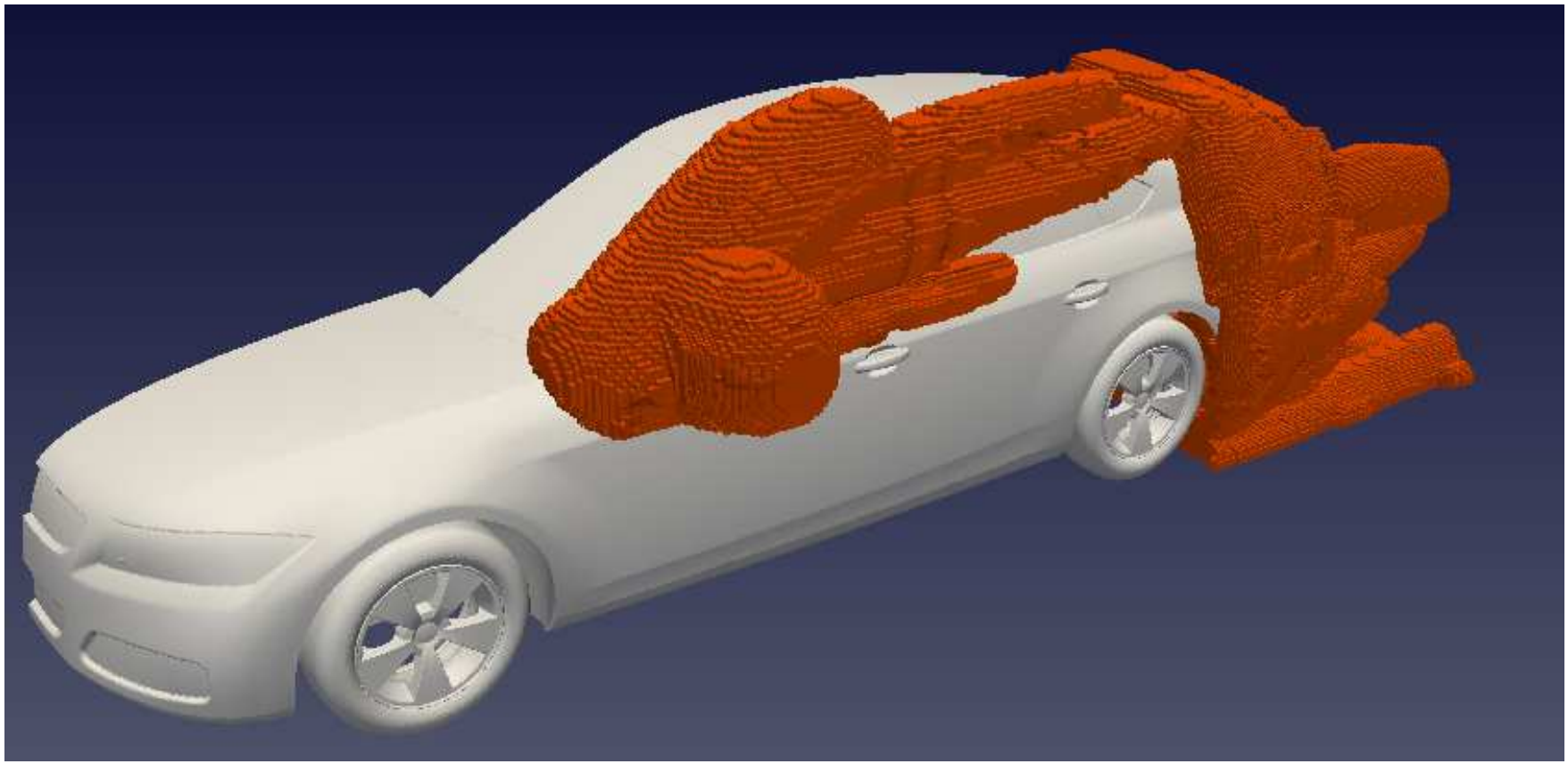

domain decomposition

Rear mirror design

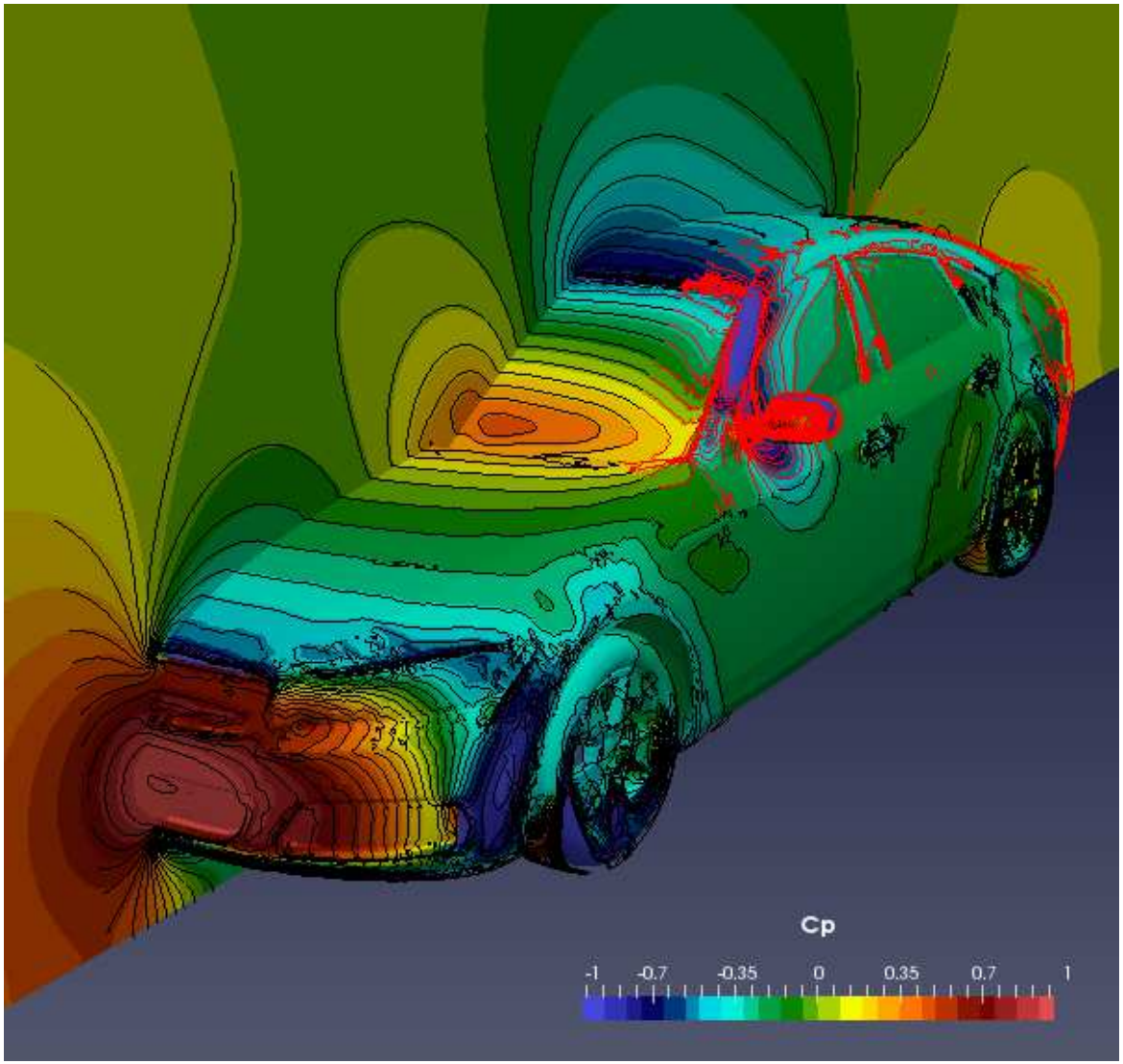

POD (black isolines) + CFD (red isolines) and full CFD solution (colormap)

Offline - Online Paradigm Perspectives

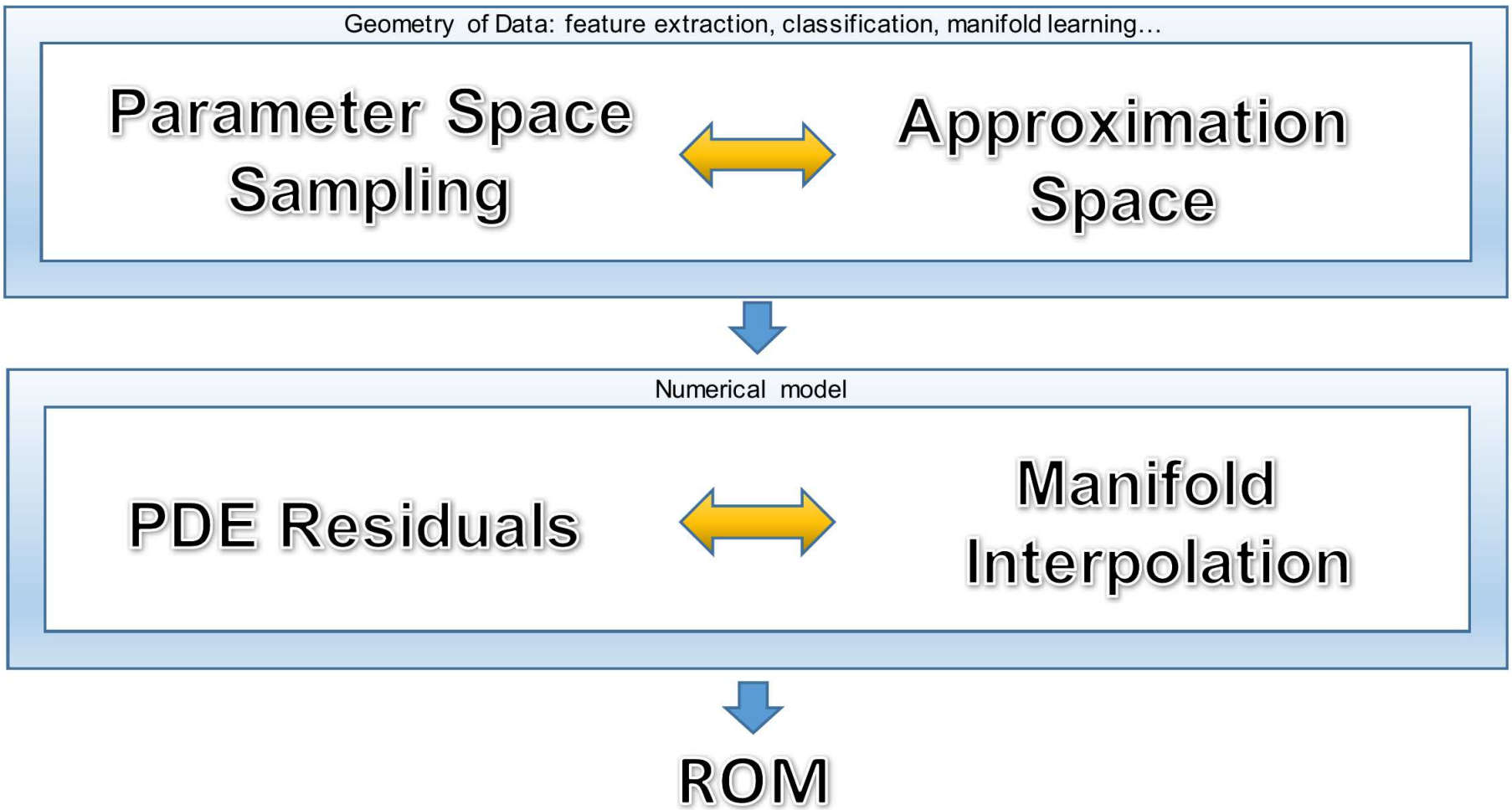

Drag coefficient

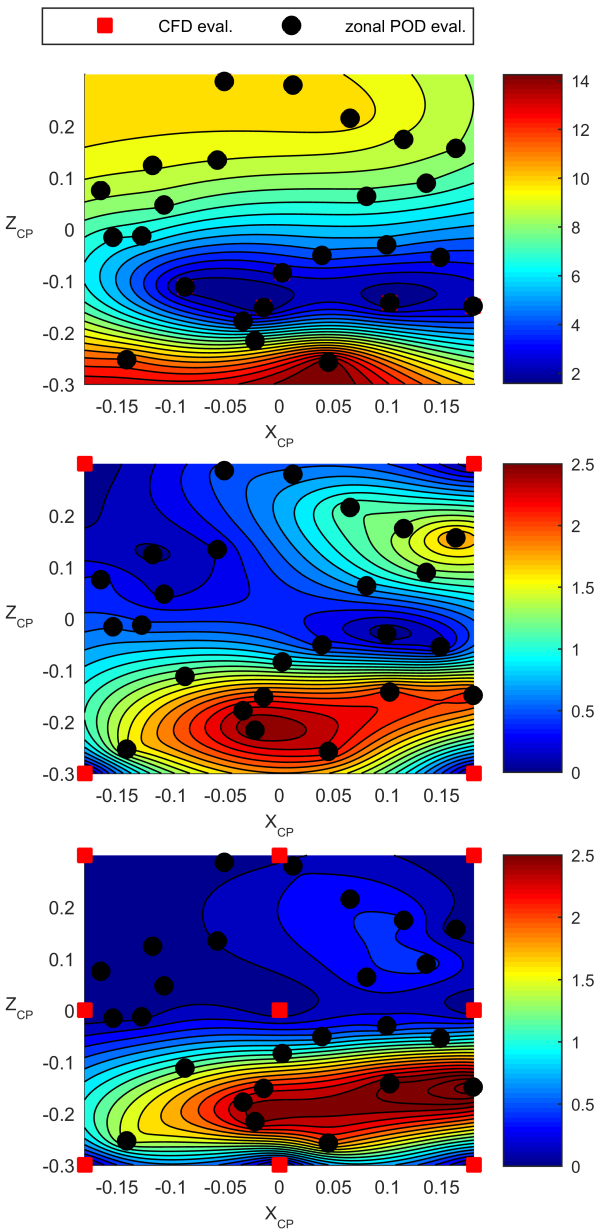

N=0
Ns=9

ε=6.9919%

N=3
Ns=4

ε=1.1263%

N=8
Ns=9

ε=0.9341%

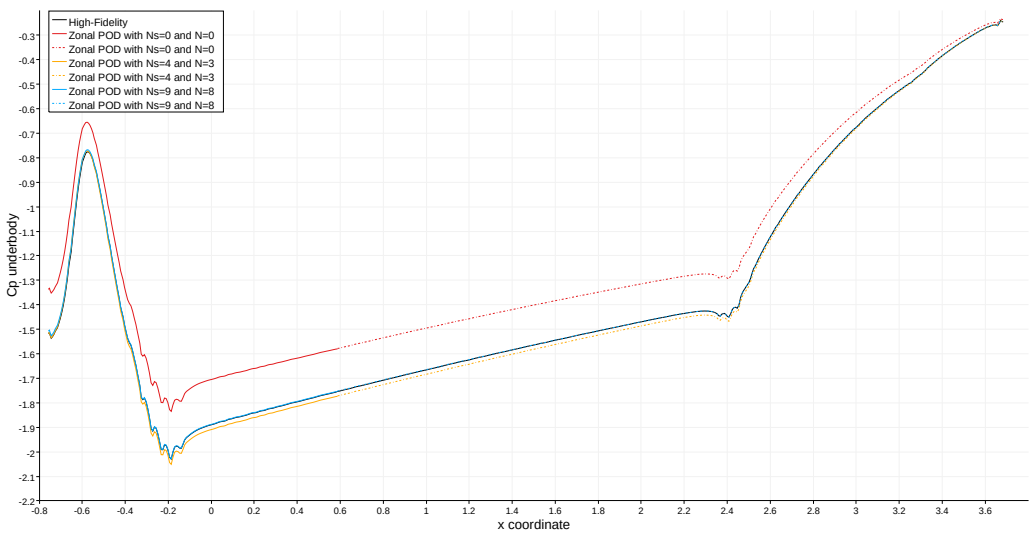

FOM/ROM coupling and LF snapshots by optimal transport

Pitching airfoil

Airbus Crank Airfoil, $k_0 = 0.04$

Inviscid flow, resolved on a fixed Cartesian grid

Database for range of oscillating frequency $k = [0.02, 5]$

9 simulations, frequency varying by factor 2

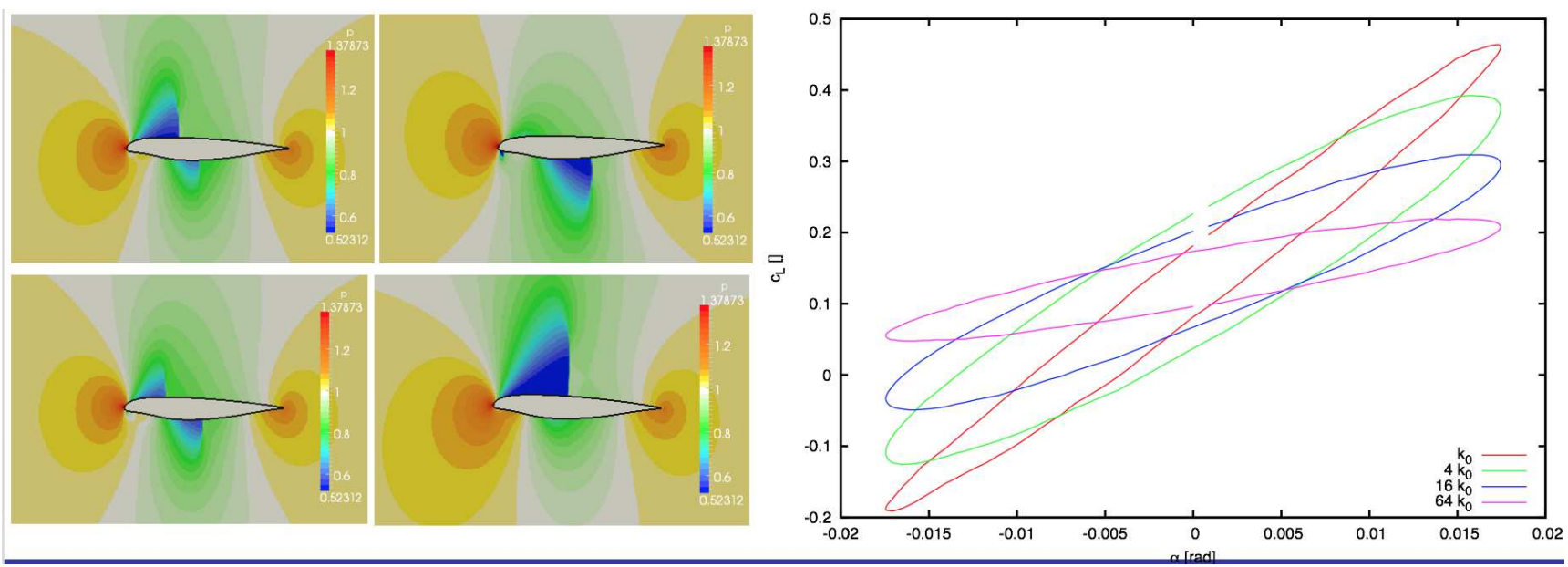

Pitching airfoil

Influence of the size of the POD domain

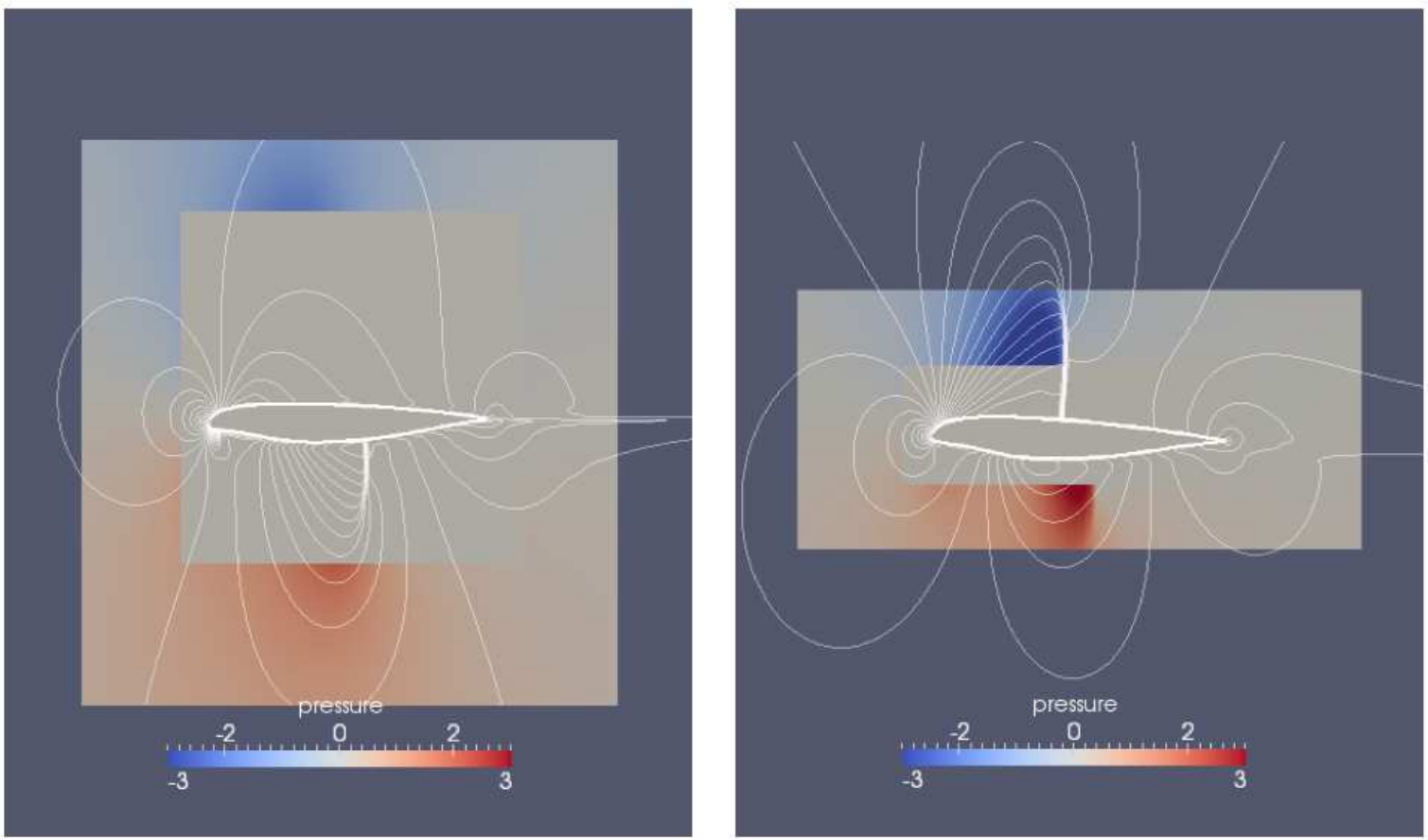

Institut de Mathématiques de Bordeaux

informatics mathematics

Pitching airfoil

Influence of the size of the POD domain

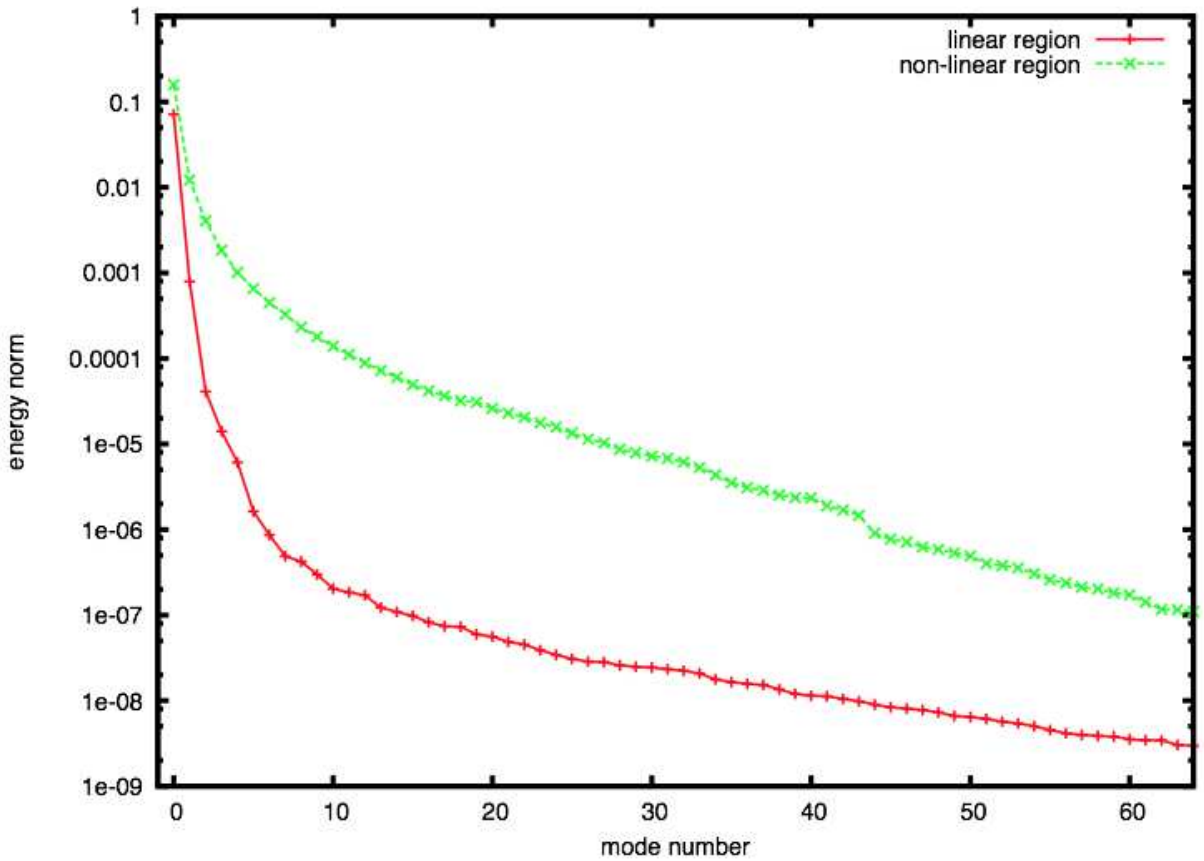

Institut de Mathématiques de Bordeaux

informatics mathematics

Pitching airfoil

Influence of the size of the POD domain: "large" FOM domain

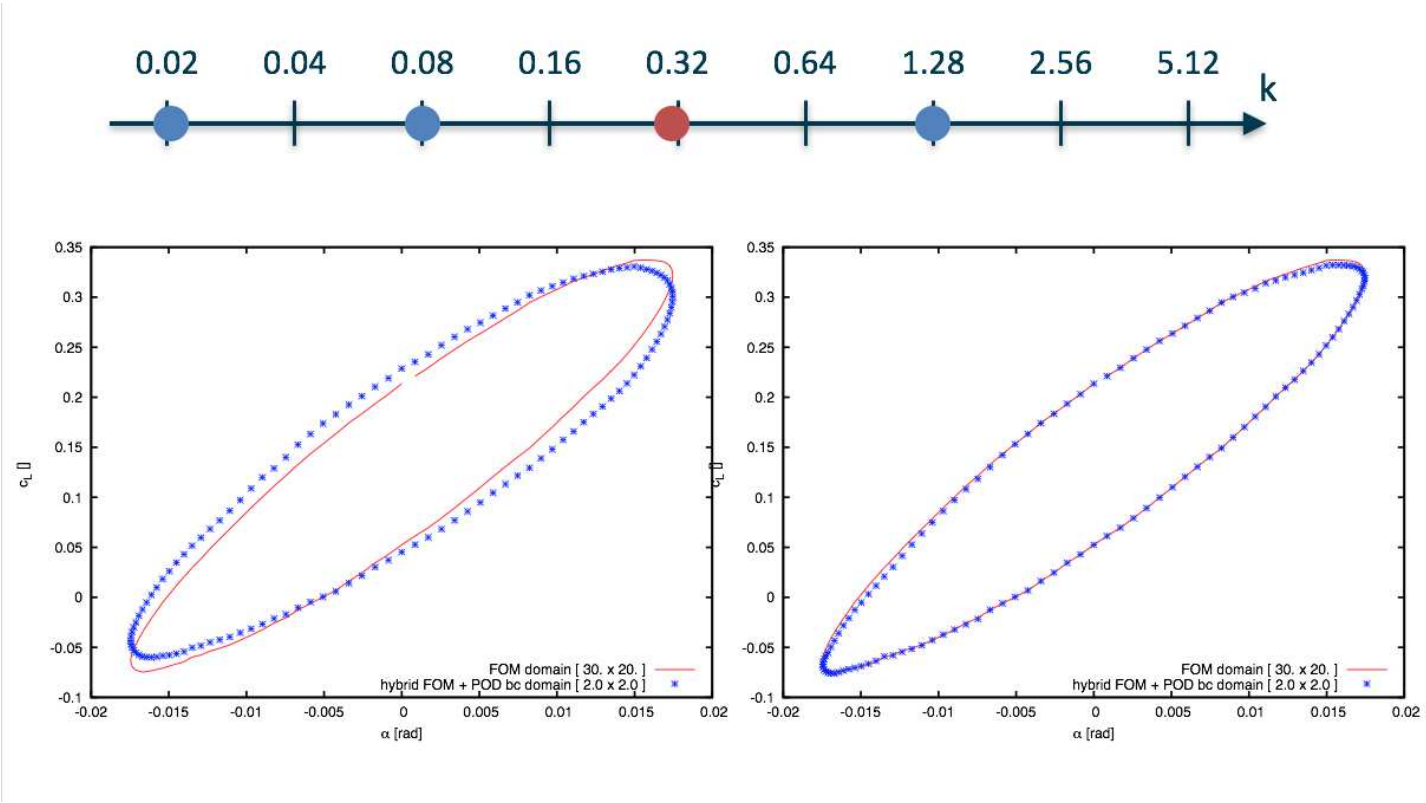

POD Basis at $k = 0.02$

Mixed POD basis at $k = 0.08$ and $k = 1.28$

Pitching airfoil

Influence of the size of the POD domain: small FOM domain

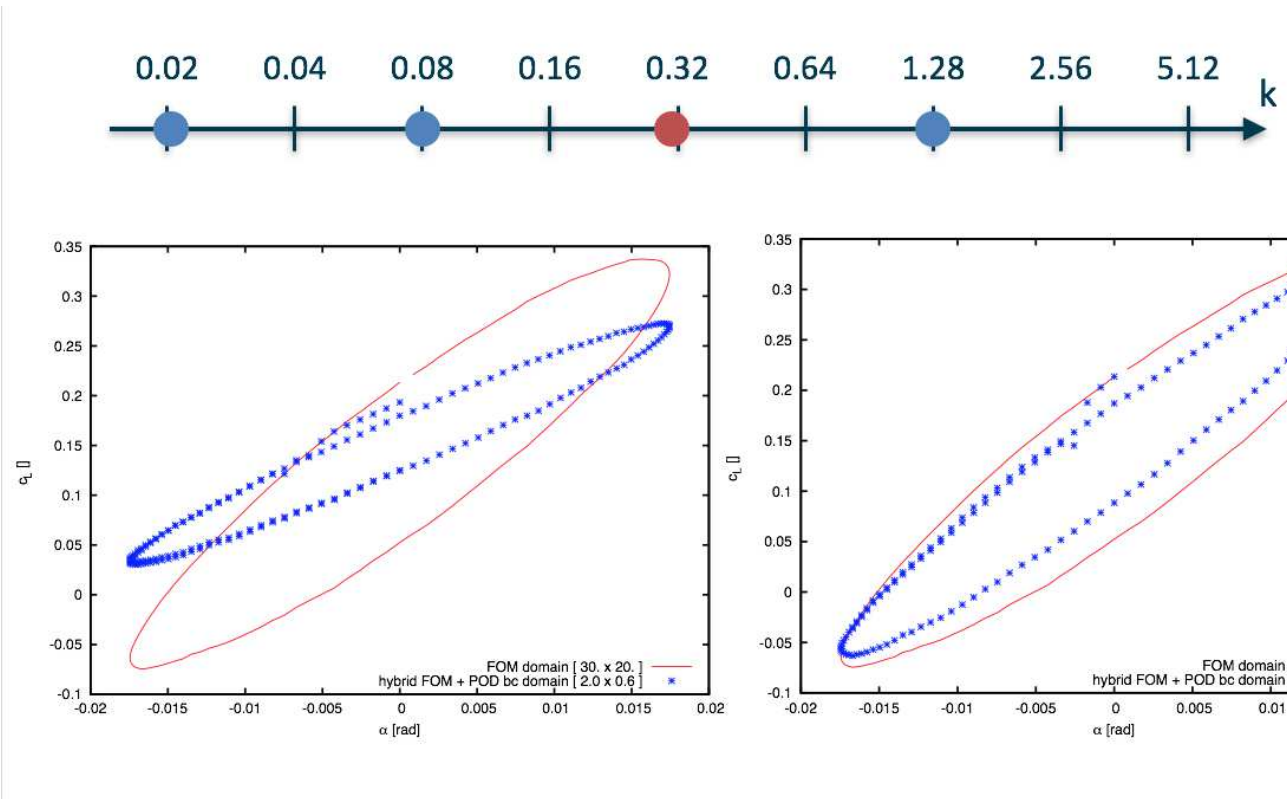

POD Basis at $k = 0.02$ Mixed POD basis at $k = 0.08$ and $k = 1.28$

Pitching airfoil

Original mixed database at $k = 0.08$ and $k = 1.28$

Pitching airfoil

Consider a given database built using snapshots at $k = 0.08$ and $k = 1.28$ (blue points)

We want to predict solution between $k = 0.08$ and $k = 1.28$, namely $k = 0.32$

We build artificial snapshots using optimal mass transportation

We enrich the database with these new snapshots

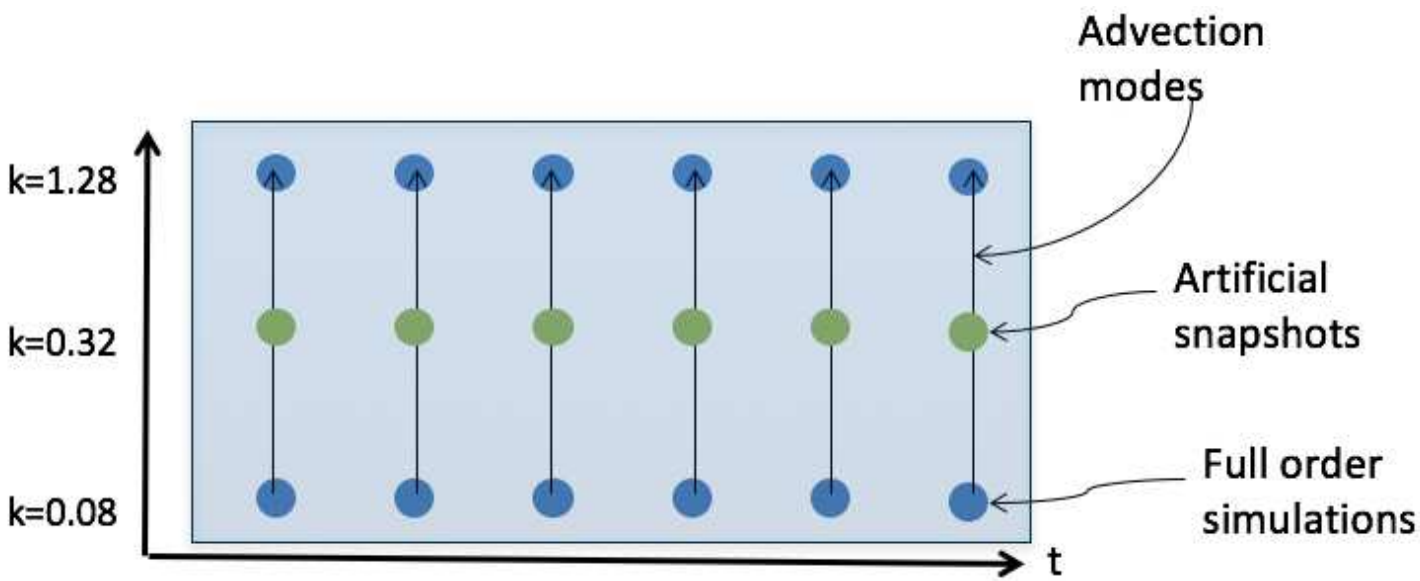

Institut de Mathématiques de Bordeaux

informatics mathematics

Pitching airfoil

Comparison between artificial snapshot and full order model

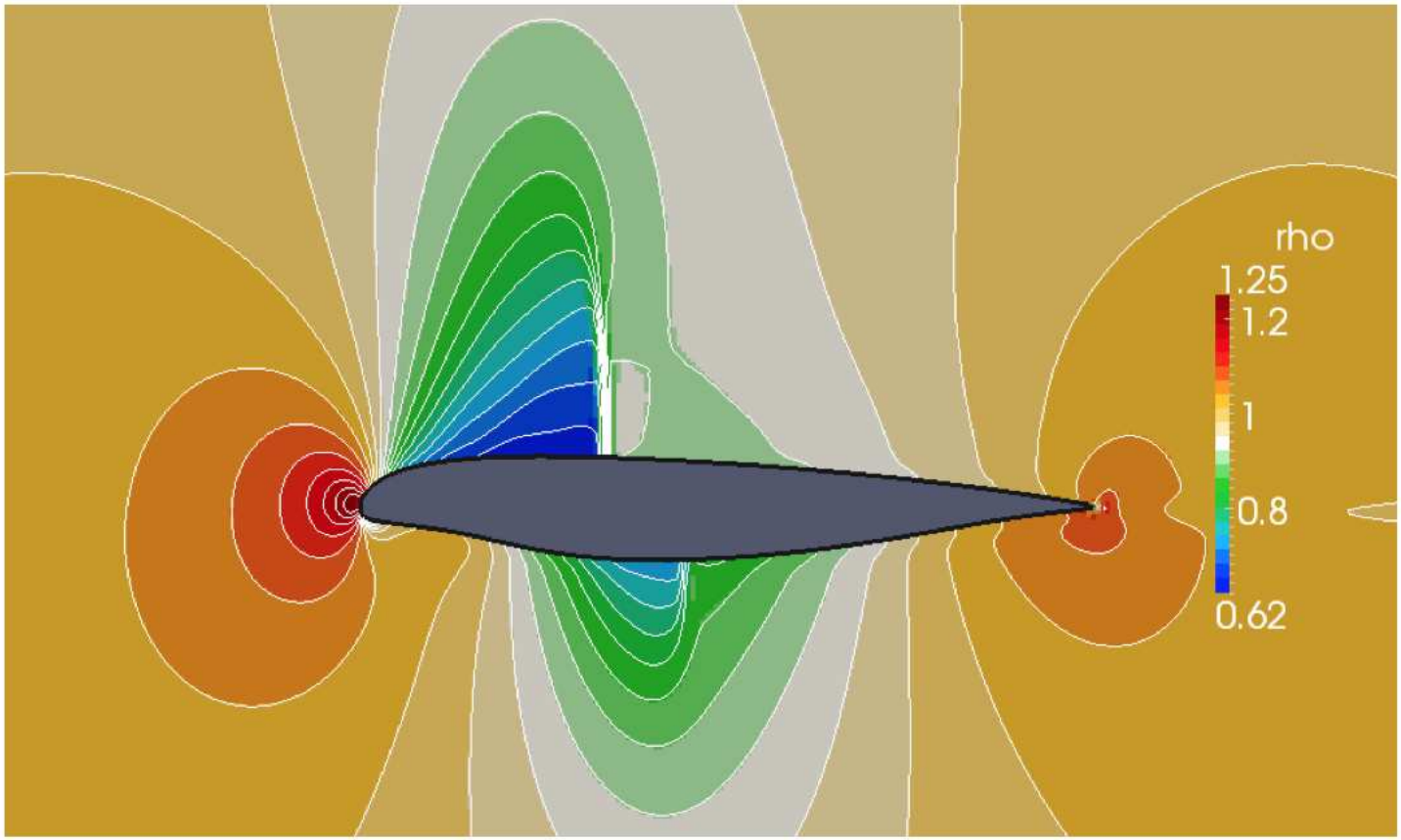

Pitching airfoil

Original mixed database
FOM at $k = 0.08$ and $k = 1.32$

Pitching airfoil

Databased enriched with artificial snapshots (without additional FOM simulations)
FOM at $k = 0.08$ and $k = 1.32$ + artificial solution at $k = 0.32$